F-box proteins MoFwd1, MoCdc4 and MoFbx15 regulate development and pathogenicity in the rice blast fungus *Magnaporthe oryzae*

Huan-Bin Shi,[1] Nan Chen,[1] Xue-Ming Zhu,[1] Shuang Liang,[1] Lin Li,[1] Jiao-Yu Wang,[2] Jian-Ping Lu (ID),[3] Fu-Cheng Lin[1*] and Xiao-Hong Liu (ID)[1*]

[1]*State Key Laboratory for Rice Biology, Biotechnology Institute, Zhejiang University, Hangzhou 310058, China.*
[2]*Institute of Plant Protection Microbiology, Zhejiang Academy of Agricultural Science, Hangzhou 310021, China.*
[3]*College of Life Sciences, Zhejiang University, Hangzhou, 310058, China.*

Summary

The Skp1-Cul1-F-box-protein (SCF) ubiquitin ligases are important parts of the ubiquitin system controlling many cellular biological processes in eukaryotes. However, the roles of SCF ubiquitin ligases remain unclear in phytopathogenic *Magnaporthe oryzae.* Here, we cloned 24 F-box proteins and confirmed that 17 proteins could interact with MoSkp1, showing their potential to participate in SCF complexes. To determine their functions, null mutants of 21 F-box-containing genes were created. Among them, the F-box proteins MoFwd1, MoCdc4 and MoFbx15 were found to be required for growth, development and full virulence. Fluorescent-microscopy observations demonstrated that both MoFbx15 and MoCdc4 were localized to the nucleus, compared with MoFwd1, which was distributed in the cytosol. MoCdc4 and MoFwd1 bound to MoSkp1 via the F-box domain, the deletion of which abrogated their function. Race tube and qRT-PCR assays confirmed that MoFwd1 was involved in circadian rhythm by regulating transcription and protein stability of the core circadian clock regulator *MoFRQ.* Moreover, *MoFWD1* also orchestrates conidial germination by influencing conidial amino acids pools and oxidative stress release. Overall, our results indicate that SCF ubiquitin ligases play indispensable roles in development and pathogenicity in *M. oryzae.*

Introduction

Rice is a staple food and provides approximately 19% of the caloric intake for half of the world's population (Elert, 2014). Rice blast disease, caused by the filamentous ascomycete *Magnaporthe oryzae* (anamorph: *Pyricularia oryzae*), poses a serious threat to rice production in fields. An annual loss of approximately 10%–30% in yield is attributed to the rice blast fungus (Talbot, 2003; Skamnioti and Gurr, 2009). Conidia, dormant structures for fungal survival and dispersal, play critical roles in the *M. oryzae* infection cycle and epidemic spread (Ebbole, 2007). Conidial germination is fine-tuned by internal physiological processes and external environmental factors such as temperature, humidity, light and nutrients (Osherov and May, 2001). The rice blast fungus initiates the infection cycle by conidial attachment to the leaf surface followed by germination upon hydration (Tucker and Talbot, 2001). Subsequently, the appressorium, a specialized infection structure, differentiates from the tip of the germ tube and facilitates penetration into the plant host. The mechanical force for plant surface penetration is transformed from high turgor pressure, up to 8 MPa, and is generated by the accumulation of an extremely high concentration of osmolytes, such as glycerol, inside the melanized appressorium (Howard *et al*., 1991). Understanding the biology of *M. oryzae* is vital for the development of new strategies to control rice blast disease. Previous research based on pharmacological and transcriptional analysis revealed that genes associated with the ubiquitin-proteasome system (UPS) played extensive roles in conidial germination. Bertomzib, a proteasome inhibitor, can inhibit conidial germination in a concentration-dependent way, indicating that the UPS plays a prominent role in initiating conidial germination in *M. oryzae* (Oh *et al*., 2012). However, the detailed mechanism underlying the control of conidial germination by UPS remains incomplete.

Ubiquitination, as a major posttranslational modification, controls many cellular processes such as the cell

cycle, transcription, protein quality control, development and differentiation, circadian clock, and signal transduction in eukaryotes (Callis, 2014). The ubiquitination of substrate protein is sequentially catalyzed via a cascade including ubiquitin activating enzyme E1, ubiquitin conjugating enzyme E2 and ubiquitin ligase E3 (Glickman and Ciechanover, 2002). Numbers of ubiquitin ligases occupy the largest proportion in the ubiquitin system and are responsible for substrate recognition (Li *et al*., 2008). Based on biochemical features and conserved domains, E3 ubiquitin ligases are divided into Really Interesting New Gene (RING) E3 ubiquitin ligases, U-box E3 ubiquitin ligases and Homologous to E6-AP Carboxyl Terminus (HECT) E3 ubiquitin ligase (Ardley and Robinson, 2005). The Skp1, Cullin1, F-box (SCF) protein E3 ubiquitin ligases are the best described group among the RING-type E3 ubiquitin ligases. The SCF complex is composed of a conserved scaffold formed by Skp1, Cul1, and Rbx1, as well as a variable F-box domain-containing protein. The F-box protein is responsible for recognizing a specific substrate. Diverse F-box proteins form a variety of SCF E3 ubiquitin ligase showing functional diversity (Cardozo and Pagano, 2004). After binding with substrates, SCF ubiquitin ligases enable the transfer of ubiquitin to substrates for ubiquitination in concert with E1 and E2 (Fig. 1A).

SCF-type E3 ubiquitin ligases regulate many biological processes in fungi by the F-box protein-mediated recognition of substrate proteins. MoSkp1, a key scaffold component of the SCF complex, is required for viability, development and pathogenicity in *M. oryzae* (Prakash *et al*., 2016). In addition, Pth1, a homologue of *Saccharomyces cerevisiae* Grr1, is the first reported F-box protein associated with pathogenicity (Sweigard *et al*., 1998). Recently, several roles were revealed in detail for MoGrr1/Pth1 in conidiogenesis and cell wall integrity in the rice blast fungus (Guo *et al*., 2015). In addition, homologous proteins for Grr1 were also reported to be important for growth, sexual development, morphogenesis and full virulence in *Cryptococcus neoformans* (Liu *et al*., 2011; Liu and Xue, 2014), *Aspergillus nidulans* (Krappmann *et al*., 2006), *Fusarium graminearum* (Han *et al*., 2007) and *Fusarium oxysporum* (Miguel-Rojas and Hera, 2016). Another F-box protein, Frp1, was found to be required for pathogenicity in *F. oxysporum* f.sp *lycopersici* (Duyvesteijn *et al*., 2005). An orthologue of *S. cerevisiae*, the F-box-containing protein Cdc4, was revealed to play vital roles in morphogenesis, cell flocculation and biofilm formation in *Candida albicans* (Atir-Lande *et al*., 2005). In *Neurospora crassa*, the F-box protein NcFwd1 participated in the regulation of the circadian clock by mediating the degradation of Frq, a key oscillator (He *et al*., 2003). The systematic analysis of *A. nidulans* using 42 F-box protein null mutants uncovered fungal-specific F-box protein, FbxA, which was required for xylanase induction and carbon
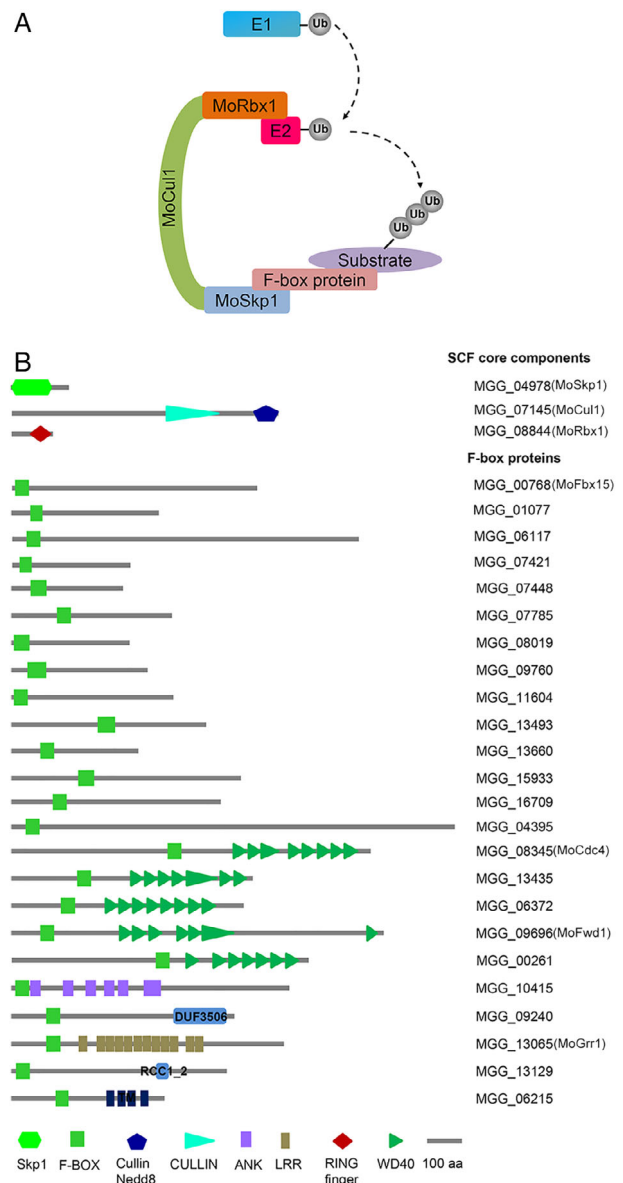

Fig. 1. Schematic of the SCF complex and associated genes in *M. oryzae*. A. Ubiquitination process mediated by the SCF complex. E1, ubiquitin activating enzyme; E2, ubiquitin conjugating enzyme; Ub, ubiquitin. B. Putative SCF complex-associated genes identified in the *M. oryzae* genome. Conserved domains predicted by the SMART web-based toolkit are shown. TM, transmembrane region. [Color figure can be viewed at wileyonlinelibrary.com]

catabolite repression (Colabardini *et al*., 2012). However, most of the SCF-type ubiquitin ligase genes have not been characterized in phytopathogenic fungi.

In this study, we conducted a comprehensive analysis of SCF-type ubiquitin ligases, revealing the potential of 17 F-box proteins to participate in an SCF complex, as well as the roles of 21 F-box proteins in growth, asexual and sexual differentiation, spore germination, appressorium formation and pathogenicity in the rice blast fungus *M. oryzae*. Among them, the novel F-box proteins MoFbx15, MoCdc4

and MoFwd1, are required for full virulence and essential for growth, conidial differentiation and germination and appressorium formation. Notably, MoFwd1 was confirmed to be involved in the circadian clock by regulating downstream *MoFRQ* expression and translation as well as conidial germination by acting on conidial amino acid pools. Our findings provide insights into SCF complex-mediated development and pathogenicity in filamentous fungi.

Results

Identification and genome-wide knockout of SCF-type ubiquitin ligase-related genes in M. oryzae

According to the previous predictions of ubiquitin pathway-associated genes in *M. oryzae*, components of the SCF-type ubiquitin ligases consist of MoSkp1 (MGG_04978), MoCul1 (MGG_07145), MoRbx1 (MGG_08844) and 24 F-box-containing proteins (Fig. 1B) (Oh *et al*., 2012). Conserved domains contained in these proteins were predicted using the SMART (http://smart.embl-heidelberg.de/) toolkit (Fig. 1B). The F-box domain was located in the N terminus of all F-box proteins. Among them, 8 F-box proteins contained other putatively substrate-interacting domains, such as Leucine Rich Region (LRR), WD40, Regulator of Chromosome Condensation 1 (RCC1) repeats, or ankyrin repeats (ANK). Seventeen genes were named after homologues genes in *S. cerevisiase*, *A. nidulans*, or *N. crassa* based on protein sequence alignment using NCBI BLASTp (Supporting Information Table S2). MGG_00768 (MoFbx15), MGG_09696 (MoFwd1), MGG_08345 (MoCdc4) and MGG_13435 (MoMet30) exhibited high similarity (41%, 58%, 59%, and 56% respectively) with their homologues Fbx15 in *A. nidulans* (Johnk *et al*., 2016), Fwd1 in *N. crassa* (He *et al*., 2003), Cdc4 in *S. cerevisiae* (Goh and Surana, 1999) and Met30 in *S. cerevisiae* (Su *et al*., 2005).

Typically, F-box proteins recruit substrates to a core ubiquitin ligase complex by binding with Skp1 (Jonkers and Rep, 2009). To ascertain whether putative F-box proteins could interact with MoSkp1 to form a protein complex, a yeast two-hybrid assay was used. Of 24 F-box proteins, the coding sequences of 19 F-box genes were cloned successfully from the wild-type strain cDNA libraries during mycelial or appressorial stages and ligated into vector pGADT7 as prey, while MoSkp1 was ligated into pGBKT7 as bait. We failed to clone the remaining five F-box genes including MGG_07421, MGG_07785, MGG_09760, MGG_13493 and MGG_15933, possibly due to low numbers of the transcripts in the mycelial or appressorial stages. As shown in Fig. 2A, except for MoFbx15 and MGG_13660, the transformants harbouring MoSkp1 and each of the above 17 F-box proteins could grow on both SD-Leu/Trp and SD-His/Leu/Trp/Ade respectively. The normal expression of the F-box proteins MoFbx15 and MGG_13660 was

confirmed in yeast transformants by western blotting (Supporting Information Fig. S1). This result indicates that 17 F-box proteins had the potential to form the SCF complex individually by binding with MoSkp1. Furthermore, to confirm that the binding is dependent on the F-box domain, truncated F-box protein mutants lacking an F-box domain, LRR or WD40 were constructed in MoGrr1, MoCdc4 and MoFwd1 (Fig. 2B). The results showed that the F-box proteins MoGrr1, MoCdc4 and MoFwd1 could no longer interact with MoSkp1 following loss of the F-box domain. However, a lack of the LRR or WD40, putative substrate binding domains, did not influence the interaction (Fig. 2C). Expression of the truncated proteins MoGrr1ΔF-box, MoFwd1ΔF-box, and MoCdc4ΔF-box, were also detected in yeast transformants by western blotting (Supporting Information Fig. S1). These data indicated that the F-box domain in the MoGrr1, MoCdc4 and MoFwd1 is indispensable for binding with MoSkp1 in the yeast two-hybrid assay. In addition, binding of MoSkp1 and MoFwd1 was further confirmed via Co-IP assay (Fig. 2D). Then, the interaction region of MoSkp1 in MoFwd1 was confirmed to be the F-box motif by an *in vitro* pull down assay (Fig. 2E).

To gain comprehensive insights into the biological functions of SCF-type ubiquitin ligases on virulence of *M. oryzae*, knockout vectors for the 27 SCF-type ubiquitin ligases-related genes mentioned previously were constructed and transformed into the wild-type strain Guy11 using the high throughput knockout system (Lu *et al*., 2014). Through two rounds of PCR verification, including the negative PCR detection of targeted genes and positive PCR detection of recombinant genomic regions (Supporting Information Fig. S2A), 21 F-box protein-encoding genes were successfully deleted with at least two independent disruption mutants for every gene. Fourteen of 21 F-box gene disruption mutants were randomly chosen and confirmed to be disrupted without ectopic insertion by Southern blotting (Supporting Information Fig. S2B and C). qPCR detection of the glufosinate resistance gene in the deletion mutants suggested that the disruptants analysed in this study contained only a single copy of the resistance gene without a random insertion of T-DNA (Supporting Information Table S2). However, core subunits including Mo*SKP1*, *MoCUL1*, *MoRBX1*, and three F-box genes, including MGG_07785, MGG_04395 (*MoFBX18*), MGG_13435 (*MoMET30*), were not successfully deleted after repeating the mutagenesis at least three times, an outcome that may be attributed to the essential roles of these genes in cell viability.

Four F-box proteins, MoFbx15, MoCdc4, MoFwd1 and MoGrr1 are important for virulence

To determine the virulence of the F-box protein deletion mutants, 5 mm-diameter mycelial plugs from Guy11 and the 21 F-box protein null mutants were inoculated on
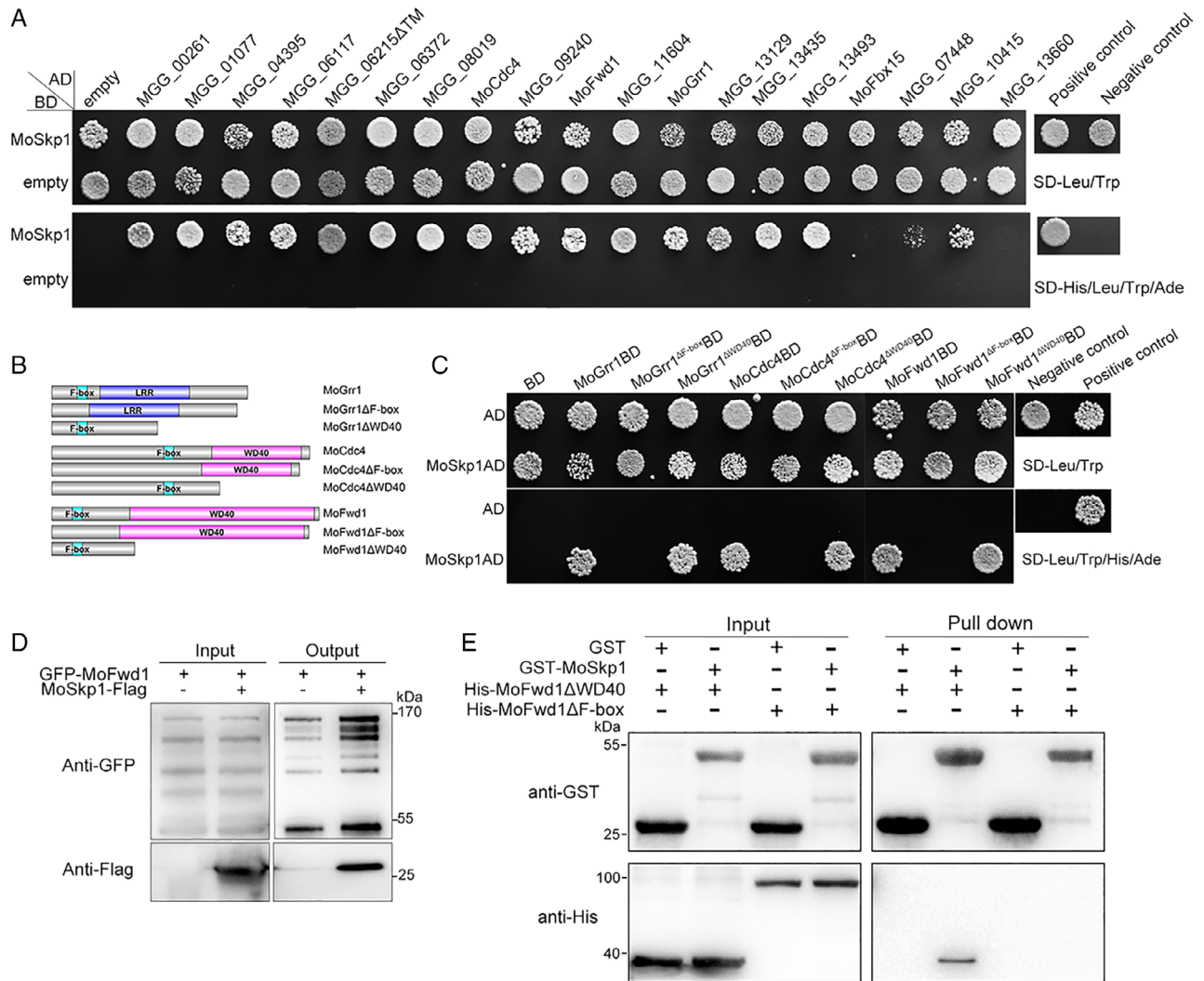
Fig. 2. The interaction between MoSkp1 and F-box domain-containing proteins. A. Yeast transformants (diluted to 1×10^6 ml^{-1}) of MoSkp1-BD and individual F-box protein-AD were cultured on SD-Leu/Trp and SD-His/Leu/Trp/Ade agar media. Plasmids pGADT7-T and pGBKT7-53 were adopted as positive control, while plasmids pGADT7-T and pGBKT7-lam used as negative control. B. Schematic presentation of truncated proteins lacking F-box domain, LRR domain or WD40 domain in MoGrr1, MoCdc4 and MoFwd1. C. Interaction between different truncated proteins and MoSkp1. D. Coimmunoprecipitation assay. Total proteins were extracted from transformants expressing GFP-MoFwd1 and transformants expressing GFP-MoFwd1 and MoSkp1-Flag followed by incubation with anti-GFP agarose beads. Eluted samples were probed with anti-Flag antibody by western blotting. E. *In vitro* pull-down assay. GST and GST fusion protein GST-MoSkp1 were purified from bacteria and incubated with cell lysates expressing His-MoFwd1ΔF-box and His-MoFwd1ΔWD40. [Color figure can be viewed at wileyonlinelibrary.com]

barley leaf explants. As shown in the Supporting Information Fig. S3, most of the null mutants imaged at 5 days post-inoculation showed similar levels of virulence in comparison to Guy11. However, Δ*Mofbx15*, Δ*Mocdc4*, Δ*Mogrr1* and Δ*Mofwd1* showed reduced disease lesion sizes. Furthermore, conidia (1×10^5 ml^{-1}) collected from Guy11 and the 21 F-box protein deletion mutants were sprayed onto rice seedlings (CO-39). Δ*Mocdc4*, Δ*Mogrr1* and Δ*Mofwd1* caused fewer lesions in comparison with Guy11, which produced a large number of typical lesions. Statistical analyses of the diseased area on the leaves were also consistent with our observations (Supporting Information Fig. S4). Other F-box deletion mutants,

including Δ*Mofbx15*, displayed a similar level of infection as Guy11 (Fig. 3A). However, microscopic observation showed that the ratios of appressorium-like structure (ALS)-mediated penetration in Δ*Mofbx15* was lower than that of Guy11 (Fig. 3B and C). The virulence assays suggested that MoFbx15, MoCdc4, MoFwd1 and MoGrr1 are important for virulence in the rice blast fungus.

To further explain the defects in the virulence of Δ*Mocdc4* and Δ*Mofwd1*, diluted conidial suspensions from Guy11, Δ*Mocdc4*, Δ*Mofwd1* and complemented strains were inoculated on detached barley leaves. The results, imaged at 5 dpi, showed that the Δ*Mocdc4* and Δ*Mofwd1* mutants caused smaller disease lesions compared with

Guy11 and the complemented strains (Fig. 3D). Microscopic observation at 48 hpi (Fig. 3E and F) confirmed that both ΔMocdc4 and ΔMofwd1 had a lower efficiency of appressorial penetration (43.5% and 0.32%) in contrast to Guy11 (77.3%) and their respective complemented strains Mocdc4c and Mofwd1c (82.6% and 84.8%), while ΔMocdc4 showed delayed invasive growth and ΔMofwd1 displayed obvious defects in mechanical penetration.

MoFWD1, MoCDC4 and MoFBX15 are involved in fungal growth and asexual development, while only MoGRR1 is involved in sexual development

To depict the reasons for reduced virulence in ΔMofbx15, ΔMocdc4 and ΔMofwd1, growth and conidiation were evaluated. As shown in Fig. 4A and Supporting Information Table S3, when cultured on complete medium plates, the disruptants of MoFWD1, MoCDC4 and MoFBX15 had an apparent reduction in vegetative growth (the diameters of

ΔMofwd1, ΔMocdc4 and ΔMofbx15 measured at 7 dpi were 4.4 ± 0.04, 4.4 ± 0.17 and 4.8 ± 0.08 mm, compared with 5.0 ± 0.03 mm of the wild-type Guy11 strain).

Conidia play an important role in the quick spread and large scale of rice blast disease epidemics in the field (Talbot, 1995). As shown in the Supporting Information Table S3, the null mutants ΔMofbx15, ΔMocdc4 and ΔMofwd1 had approximately 90% or greater reduction in conidiation in contrast with the wild-type strain (specifically $(7.3 \pm 3.8) \times 10^4$ plate^{-1}, $(2.0 \pm 0.9) \times 10^4$ plate^{-1} and $(0.6 \pm 0.1) \times 10^4$ plate^{-1}, respectively, relative to $(90.8 \pm 27.5) \times 10^4$ plate^{-1} in the wild type). Microscopic observations revealed that few conidiophores had differentiated in ΔMofbx15, ΔMocdc4 and ΔMofwd1, and only a few conidia hung on the conidiophores of these strains in comparison with Guy11 and their complemented strains (Fig. 4B). Although the conidia from Guy11, ΔMofbx15, ΔMocdc4 and ΔMofwd1 did not show significant differences in length and width (Supporting Information Table S3), the conidia of
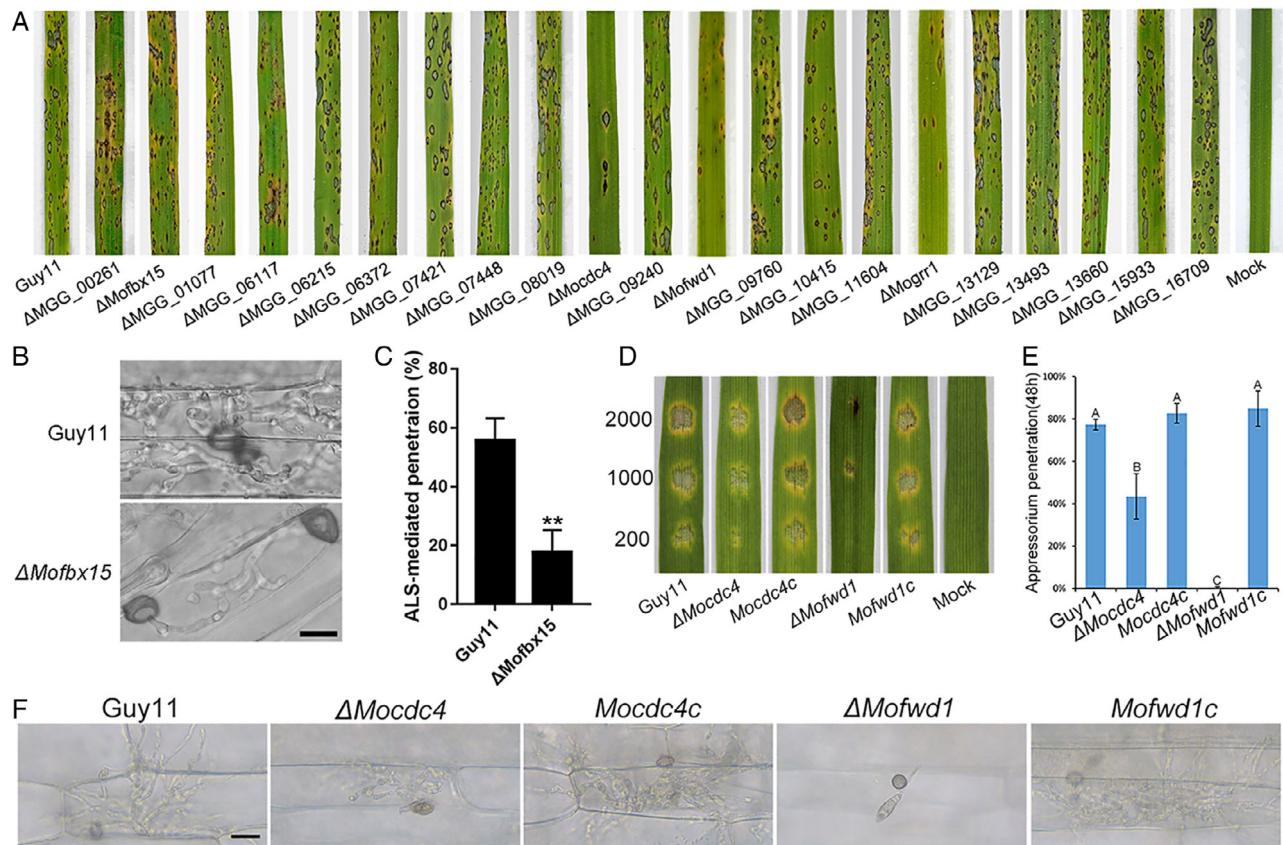

Fig. 3. F-box proteins are required for full virulence in *M. oryzae*. A. Rice leaves spray-inoculated with conidia collected from F-box protein null mutants. The picture was taken at 4–5 dpi. B. ALS-mediated penetration on barley leaves at 48 hpi. A small piece of marginal regions from Guy11 and ΔMofbx15 colonies were cut and inoculated on barley leaves. Microscopic observation was carried on after the leaves were decoloured. C. Ratio of ALS-mediated penetration. Asterisk (*) indicates significant at ($P < 0.01$). D. A fixed number of conidia from Guy11, ΔMocdc4, ΔMofwd1, and complemented strains were dropped on barley leaves. Pictures were captured at 5 dpi. E. Ratios of the appressorium penetration of Guy11, ΔMocdc4, ΔMofwd1 and complemented strains. F. Conidia from the wild-type, ΔMocdc4, ΔMofwd1, and complemented strains were inoculated on barley leaves *in vitro*. Microscopic observations were conducted at 48 hpi following leaf decolouration. Error bars indicate standard deviation. The data were analysed by Duncan's test ($P < 0.01$), and columns labelled with the same letter indicate no significant difference. Bar = 20 μm. [Color figure can be viewed at wileyonlinelibrary.com]
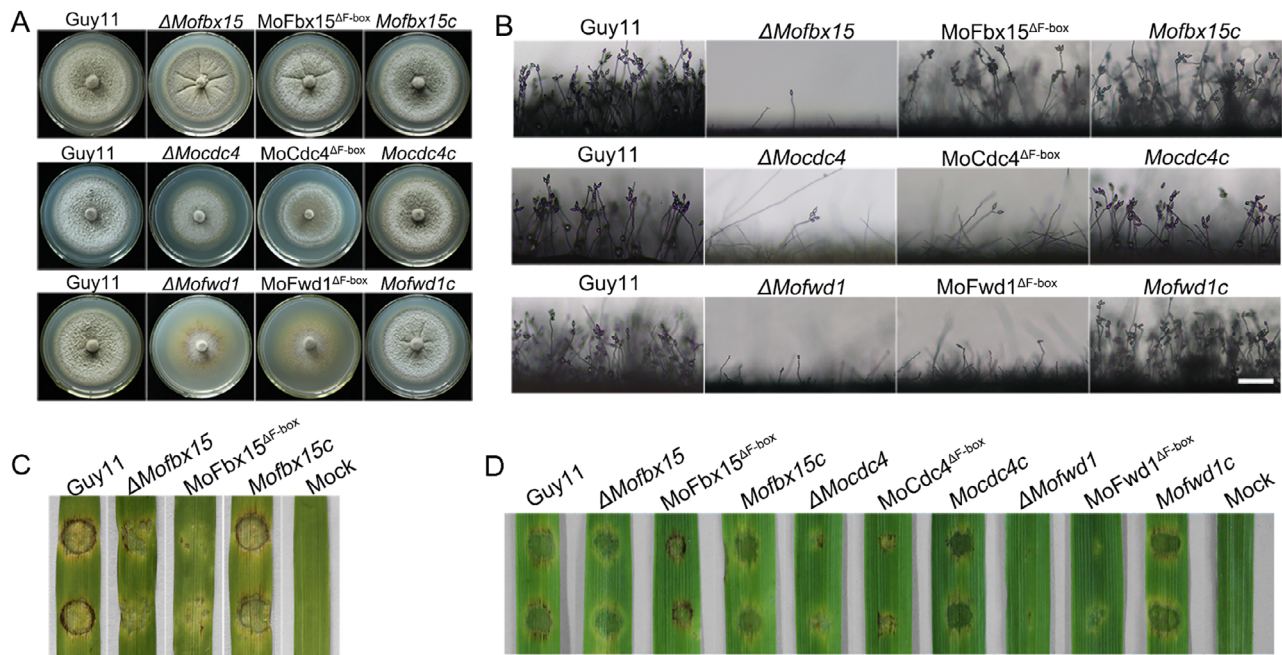
Fig. 4. Functional analysis of the F-box domain in MoFbx15, MoCdc4 and MoFwd1. A. Colony morphology of the wild-type, Δ*Mofbx15*, MoFbx15$^{ΔF-box}$, Δ*Mocdc4*, MoCdc4$^{ΔF-box}$, Δ*Mofwd1*, MoFwd1$^{ΔF-box}$ and complemented strains. Pictures were taken at 7 dpi. B. Microscopic observation of conidiophore. Conidiophores were induced under constant light and observed at 24 hpi. Bar = 100 μm. C. Virulence of the wild-type, Δ*Mofbx15*, MoFbx15$^{ΔF-box}$ and complemented strain Mofbx15c. Mycelial plugs were inoculated on barley leaves and pictures were taken at 5 dpi. D. Virulence of the wild-type, Δ*Mofbx15*, MoFbx15$^{ΔF-box}$, Δ*Mocdc4*, MoCdc4$^{ΔF-box}$, Δ*Mofwd1*, MoFwd1$^{ΔF-box}$ and complemented strains. Twenty microliters of conidial drops were inoculated on barley leaves. Pictures were taken at 5 dpi. [Color figure can be viewed at wileyonlinelibrary.com]

Δ*Mocdc4* showed an obvious increase in the proportion of two-celled conidia in contrast to those of Guy11 and the complemented strain *Mocdc4c* (Supporting Information Fig. S5).

Previous reports indicated that the ubiquitin system is involved in sexual development of *M. oryzae* because the deletion of MGG_01282, which encodes a polyubiquitin, resulted in female sterility (Oh *et al.*, 2012). Due to that finding, sexual development was also evaluated by cross-culturing Guy11, Δ*Mofbx15*, Δ*Mogrr1*, Δ*Mocdc4* and Δ*Mofwd1* with the opposite mating type strain 2539. Supporting Information Figure S6 shows that Δ*Mofbx15*, Δ*Mogrr1*, Δ*Mocdc4*, Δ*Mofwd1* and Guy11 disruptants can produce asci with ascospores. Given that the homologue of Grr1 in *Gibberella zeae*, Fbp1, is more important for sexual development in the female mating type than in the male mating type (Ardley and Robinson, 2005), *MoGRR1* was knocked out in the 2539 strain to determine if *GRR1* plays the same role in *M. oryzae*. The fertility of the resultant null mutant's was determined by cross-culturing it with wild-type Guy11 and the Δ*Mogrr1* null mutant in the Guy11 genetic background. Interestingly, no asci were produced in either outcrossing (Supporting Information Fig. S6), indicating that MoGrr1 in the female mating type is critical for fertility regardless of the male genotype, while the loss of fertility through the deletion of *MoGRR1* in the male mating types can be partially restored through mating with a female that carries a functional copy.

The F-box proteins MoFwd1, MoCdc4 and MoFbx15 are required for conidial germination and appressorial formation

The early development process conidial germination plays vital roles in the efficiency of plant infection. We calculated the conidial germination of *MoFWD1*, *MoCDC4* and *MoFBX15* gene disruptants and the wild-type strain at 4 h post incubation (hpi). Δ*Mofbx15*, Δ*Mocdc4* and Δ*Mofwd1* displayed an obvious delay in germination in contrast to that of Guy11 (the germination ratios were 80.1 ± 1.2%, 24.3 ± 8.4% and 6.9 ± 3.2% relative to 98.5 ± 0.4% of Guy11). Among them, the loss of MoFwd1 caused the most severe defects of germination. Reintroduction of the *MoFWD1* wild-type allele into Δ*Mofwd1* restored the germination rate to a level similar to that of Guy11 (Supporting Information Table S3).

The appressorium is a specialized infection structure used by *M. oryzae* for penetration and colonization of the rice leaf (Bourett and Howard, 1990). We evaluated the effects of *MoFBX15*, *MoCDC4* and *MoFWD1* on appressorial formation. The disruption of *MoCDC4* and *MoFWD1* resulted in a significant reduction of appressorium formation (the ratios of appressorial formation were 6.6 ± 2.3% and 5.9 ± 0.5% in contrast to 98.7 ± 1.9% of Guy11 and 96.0 ± 2.5% of Δ*Mofbx15*) (Supporting Information Table S3). These data indicated that the virulence defects in Δ*Mofbx15*, Δ*Mocdc4* and Δ*Mofwd1* were

partially due to impairments of conidial germination and appressorial formation.

The F-box domain plays key roles in development and plant infection

To better determine the potential roles of the F-box domain, F-box domain deletion constructs MoCdc4$^{\Delta F\text{-box}}$, MoFwd1$^{\Delta F\text{-box}}$ and MoFbx15$^{\Delta F\text{-box}}$ were transformed into $\Delta Mocdc4$, $\Delta Mofwd1$ and $\Delta Mofbx15$ respectively. The expression of the MoCdc4$^{\Delta F\text{-box}}$, MoFwd1$^{\Delta F\text{-box}}$ and MoFbx15$^{\Delta F\text{-box}}$ was verified by qPCR (Supporting Information Fig. S7). As shown in Fig. 4 and in the Supporting Information Table S3, the MoFwd1$^{\Delta F\text{-box}}$ transformant did not display significant differences in growth, conidiation and virulence if compared to the respective deletion mutant. On the contrary, the percentage of conidial germination and appressorium formation in the MoCdc4$^{\Delta F\text{-box}}$ transformant (34.3 ± 2.7%, 37.0 ± 7.8%) had a distinct increase over those of $\Delta Mocdc4$ (24.3 ± 8.4%, 6.6 ± 2.3%), although the ratios were still lower than those of the wild type (98.5 ± 0.4%, 98.7 ± 1.9%). The MoFbx15$^{\Delta F\text{-box}}$ mutant had a restoration in growth, conidiation and germination in comparison to $\Delta Mofbx15$, but these levels were lower than those in Guy11. These results indicated that the F-box domain plays a functional role in development and virulence in *M. oryzae*, but its importance varies with different F-box proteins.

Expression patterns and localization of MoFbx15, MoCdc4 and MoFwd1

Dynamic changes in gene expression levels have a close association with fungal development and differentiation (Takano *et al*., 2003; Oh *et al*., 2008). Expression levels of *MoFBX15*, *MoCDC4* and *MoFWD1* were measured in total RNA extracts from five developmental stages, including vegetative hyphae, conidia, mature appressoria (18 h), invasive hyphae and nitrogen-starved mycelia. Figure 5A showed that the expression of *MoFBX15* was significantly upregulated (more than fivefold) during the invasive hyphal stage compared with the other four stages. No significant difference in the expression levels of *MoCDC4* was detected over the five different stages tested, while the expression of *MoFWD1* showed a greater than twofold increase in the invasive hyphal stage compared with its expression in the conidial and appressorial stages. Altogether, the F-box proteins showed differential expression patterns.

The localization of MoFbx15, MoCdc4, and MoFwd1 was observed by tagging with eGFP at the nitrogen terminus or carbon terminus of their peptidic sequences. Three fusion constructs, GFP-MoFwd1, MoCdc4-GFP and MoFbx15-GFP, were generated and transformed into null mutants of

$\Delta Mofwd1$, $\Delta Mocdc4$ and $\Delta Mofbx15$ respectively. Predictions from the cNLS Mapper program (http://nls-mapper.iab. keio.ac.jp/cgi-bin/NLS_Mapper_form.cgi/) suggested that MoCdc4 is a nuclear protein with two hypothetical nuclear localization signals (NLS), ^{556}KRKR^{559} and ^{570}KRR^{572}. Fluorescent-microscopy observation showed that eGFP-labelled MoCdc4 displayed dotted fluorescent signals and colocalized with Hoechst-stained nuclei in apical hyphae (Fig. 5C). Further, the localization of the protein did not change when the F-box domain was deleted (Fig. 5C). Unexpectedly, eGFP-labelled MoFbx15 also localized to the nucleus in the hyphal stage (Fig. 5B) and during the development of an appressorium (Supporting Information Fig. S8). On the contrary, GFP-MoFwd1 signals were distributed in the cytosol of vegetative hyphae (Fig. 5D) and invasive hyphae (Supporting Information Fig. S9) with punctate spots during these two stages. These results suggested that diverse F-box protein localization patterns may contribute to efficient intracellular coordination of substrate degradation and regulation of specific cellular processes in *M. oryzae.*

MoFwd1 is involved in regulating circadian rhythm

In *N. crassa*, NcFwd1 plays an essential role in regulating the circadian clock by recognizing and degrading a core circadian regulator, Frq (Fig. 6A) (Montenegro-Montero *et al*., 2015). To determine whether MoFwd1 is involved in the regulation of the circadian clock in *M. oryzae*, a race tube assay was used. After cultivation in constant darkness for 14 days, no circadian changes were observed in Guy11, $\Delta Mofwd1$ and the complemented strain *MoFwd1c.* When transitioned to cycles of 12 h-light/12 h-dark, clear bands could be observed in Guy11 and *MoFwd1c*, implying the presence of a functional circadian response in these fungi. However, no obvious bands were observed in $\Delta Mofwd1$ (Fig. 6B), indicating that circadian rhythm was disturbed in $\Delta Mofwd1.$

The circadian clock in *N. crassa* is regulated by a negative feedback regulatory mechanism in which Fwd1 ubiquitylates and degrades Frq to release inhibition of the upstream transcriptional factors WC-1 and WC-2, which promote *FRQ* transcription (Fig. 6A) (Montenegro-Montero *et al*., 2015). Due to the loss of circadian rhythm in the *MoFWD1* deletion mutant, we presumed that the circadian oscillation of *MoFRQ* mRNA may be affected in the *MoFWD1* null mutant. To confirm this, the expression levels of *MoFRQ* were examined in mycelia cultured under conditions of constant dark or alternating light/dark cycles. As shown in Fig. 6D, under constant darkness, the expression pattern of *MoFRQ* still showed a circadian rhythm in both the wild-type strain and the $\Delta Mofwd1$ null mutant, indicating that MoFwd1 is not necessary for the rhythmic transcription of *MoFRQ.* However, under light/dark
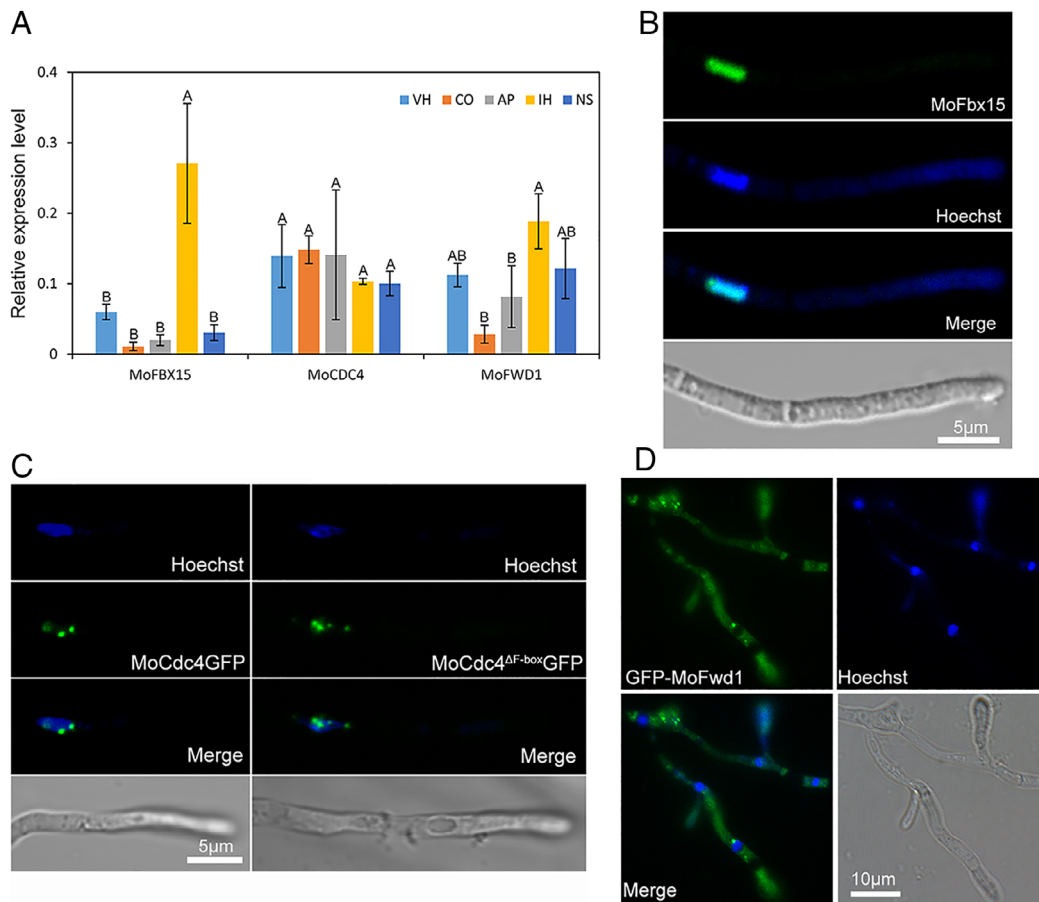
Fig. 5. Expression patterns and intracellular localization of MoFbx15, MoCdc4 and MoFwd1. A. Dynamics in the transcriptional levels of *MoFBX15*, *MoCDC4* and *MoFWD1* during vegetative hyphae (VH), conidia (CO), appressoria (AP), infectious hyphae (IH) and nitrogen-starvation treated mycelia (NS). *β-tubulin* was used as the reference gene, and the error bars represent standard deviation. Significant differences were annotated by different letters via Duncan's test (*P* < 0.01). B. MoFbx15GFP signals were localized to the nucleus in the hyphal stage. C. MoCdc4GFP and MoCdc4$^{\Delta F-box}$GFP signals were detected in Hoechst-stained nuclei in apical hyphae. D. Fluorescence of GFP-MoFwd1 was distributed in the cytoplasm of vegetative hyphae. Bars were annotated in indicated pictures. [Color figure can be viewed at wileyonlinelibrary.com]

transition conditions, the mRNA levels of *MoFRQ* in the wild-type strain had an obvious upregulation upon light induction compared with that of the Δ*Mofwd1* null mutant (Fig. 6C), suggesting that MoFwd1 could affect the transcription of *MoFRQ* in response to stimulation by illumination.

To determine whether MoFwd1 participates in the degradation of MoFrq, a fusion protein GFP-MoFrq was introduced into Guy11 and Δ*Mofwd1* and analyzed by Western blot. As shown in Fig. 6E, the fusion protein GFP-MoFrq could be detected in Δ*Mofwd1* but was degraded in Guy11, suggesting that MoFwd1 was involved in the stability of MoFrq. The expression levels of GFP-MoFrq in Guy11 and Δ*Mofwd1* were comparable (Figs. 6F and G). Constitutive expression of GFPMoFrq in Δ*Mofwd1* did not restore defects in growth, conidiation, conidial germination and appressorium formation of Δ*Mofwd1* but partially rescued virulence on barley leaves when inoculated with mycelial plugs (Supporting Information Fig. S10). According to our results, we assume that MoFwd1 modulates the transcription of *MoFRQ* and the protein degradation of MoFrq.

To further depict the functional roles of *MoFWD1* in development and virulence, its downstream target *MoFRQ* downstream was knocked out (Supporting Information Fig. S2A). Phenotypic analysis showed that the disruption of *MoFRQ* caused slow growth, reduced conidiation (the relative conidiation ratios were 3.5% and 4.3% in Δ*Mofrq*-2 and Δ*Mofrq*-3 in contrast to 100% of Guy11), delayed conidial germination (14.5% and 8.6% in Δ*Mofrq*-2 and Δ*Mofrq*-3 in contrast to 88.4% of Guy11 at 4 hpi), decreased appressorial formation (18.6% and 16.9% in Δ*Mofrq*-2 and Δ*Mofrq*-3 in contrast to 89.4% of Guy11 at 24 hpi) and reduced virulence (Fig. 7), similar to the defects in Δ*Mofwd1*, suggesting that *MoFWD1* is involved in development and virulence by mediating the light-induced transcription of *MoFRQ*.
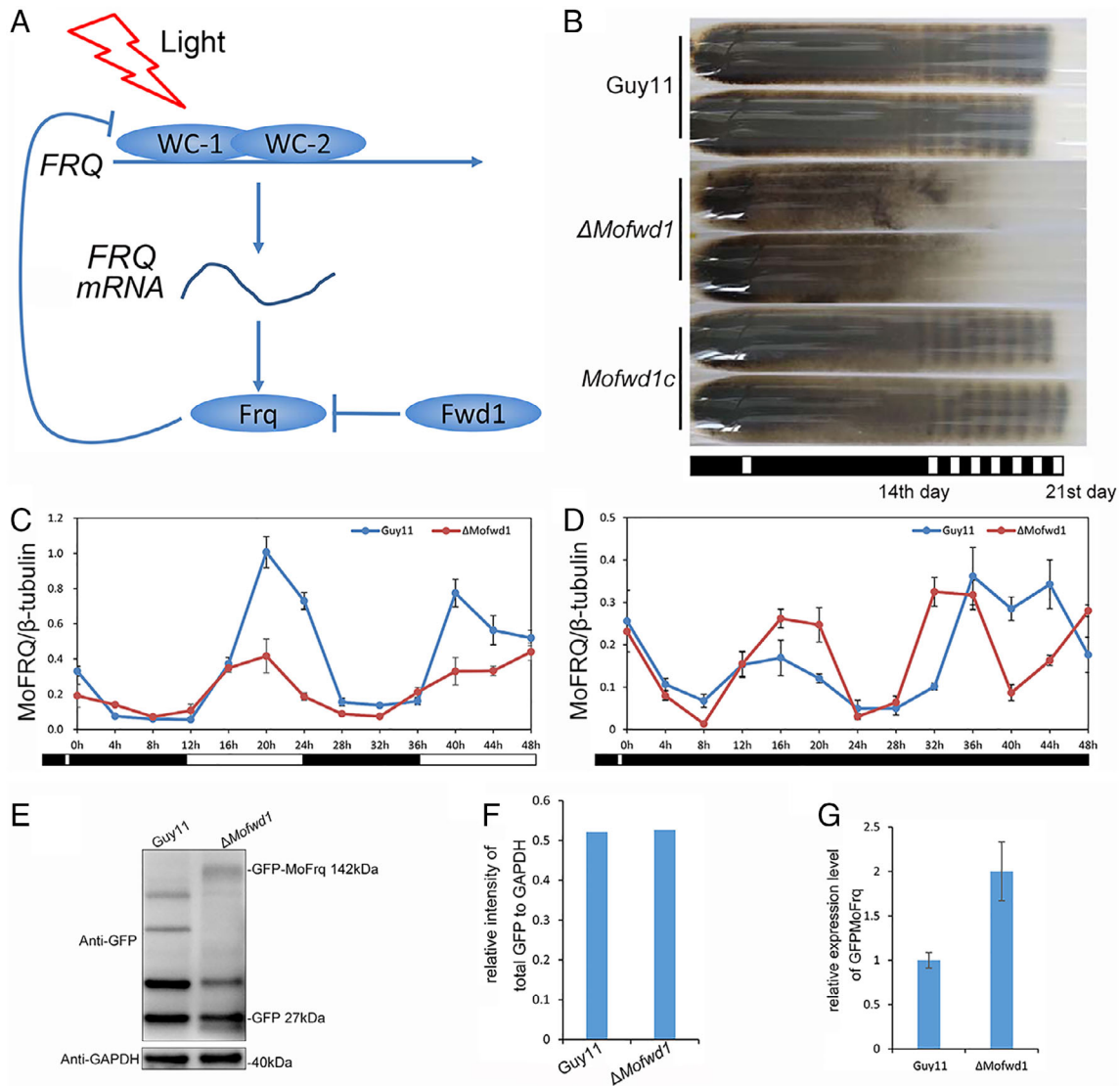
Fig. 6. MoFwd1 is involved in circadian rhythm by mediating expression and degradation of MoFrq. A. Schematic of the mechanism underlying the circadian clock in *N. crassa*. B. Race tube assay. The Guy11, Δ*Mofwd1*, and complemented strains were cultured in constant darkness followed by 30 min light and then transitioned to dark for 2 weeks and light/dark cycles for another week. C. Expression of *MoFRQ* under conditions of light/dark transition. D. Expression of *MoFRQ* in constant darkness. The wild-type strain and Δ*Mofwd1* were cultured in complete medium and sampled at the time points indicated respectively. Error bars show standard deviation. E. Western blot detection of GFPMoFrq in the wild type and Δ*Mofwd1*. The fusion protein GFPMoFrq was expressed in the wild type and Δ*Mofwd1* and a protein of the predicted molecular weight was detected in Δ*Mofwd1*. Protein expression levels (F) and transcriptional levels (G) were determined in Guy11 expressing GFP-MoFrq and Δ*Mofwd1* expressing GFP-MoFrq. [Color figure can be viewed at wileyonlinelibrary.com]

MoFwd1 regulates germination by the maintenance of conidial amino acid pools

The cAMP-PKA signalling pathway has been shown to participate in regulating conidial germination (Osherov and May, 2001). To determine whether MoFwd1 is associated with the activation of cAMP-PKA signalling, exogenous cAMP was added to conidial drops of Guy11 and Δ*Mofwd1*. As shown in Fig. 8A, the percentage of conidial germination in Δ*Mofwd1* increased from 8.6% to 38.6% at 4 hpi, and from 30% to 74.5% at 24 hpi, suggesting that

MoFwd1 may be associated with the cAMP-PKA signalling pathway.

In addition to environmental factors such as proper temperature, and the availability of water, oxygen and nutrients such as glucose, amino acids and inorganic salts are also required for conidial germination in some filamentous fungi (Osherov and May, 2001). However, conidia in *M. oryzae* can germinate in nutrient-free conditions, mainly depending on intracellular stored nutrients. We thus hypothesized that delayed germination in the Δ*Mofwd1* mutant may be caused by defects in the

accumulation of nutrients. To test this, conidia from Guy11 and ΔMofwd1 were suspended in sterile distilled water, 2.5% glucose, or complete media and subsequently incubated on a hydrophobic surface. As shown in Fig. 8A, for ΔMofwd1 at 4 hpi, the percentage of conidial germination in complete media (44.3 ± 8.2%) obviously increased over germination in sterile distilled water (8.6 ± 3.6%), whereas the percentage of germination in 2.5% glucose (15.2 ± 3.6%) did not display a significant difference with that in sterile distilled water. At 24 hpi, the germination percentage of ΔMofwd1 in 2.5% glucose (41.8 ± 4.8%) and in complete media (93.2 ± 5.5%)

showed significant differences with germination in sterile distilled water (30.1 ± 3.1%), and the percentage of successful germination in complete media were as high as those of the wild type. These data suggested that exogenous nutrients could complement the germination defects in ΔMofwd1.

The complete medium is a complex synthetic medium comprised of many ingredients, including sources of nitrogen, carbon and inorganic salts (Parker *et al.*, 2008). To dissect which components of the complete medium function in triggering germination, solutions of individual components, including amino acids, sodium nitrate, trace
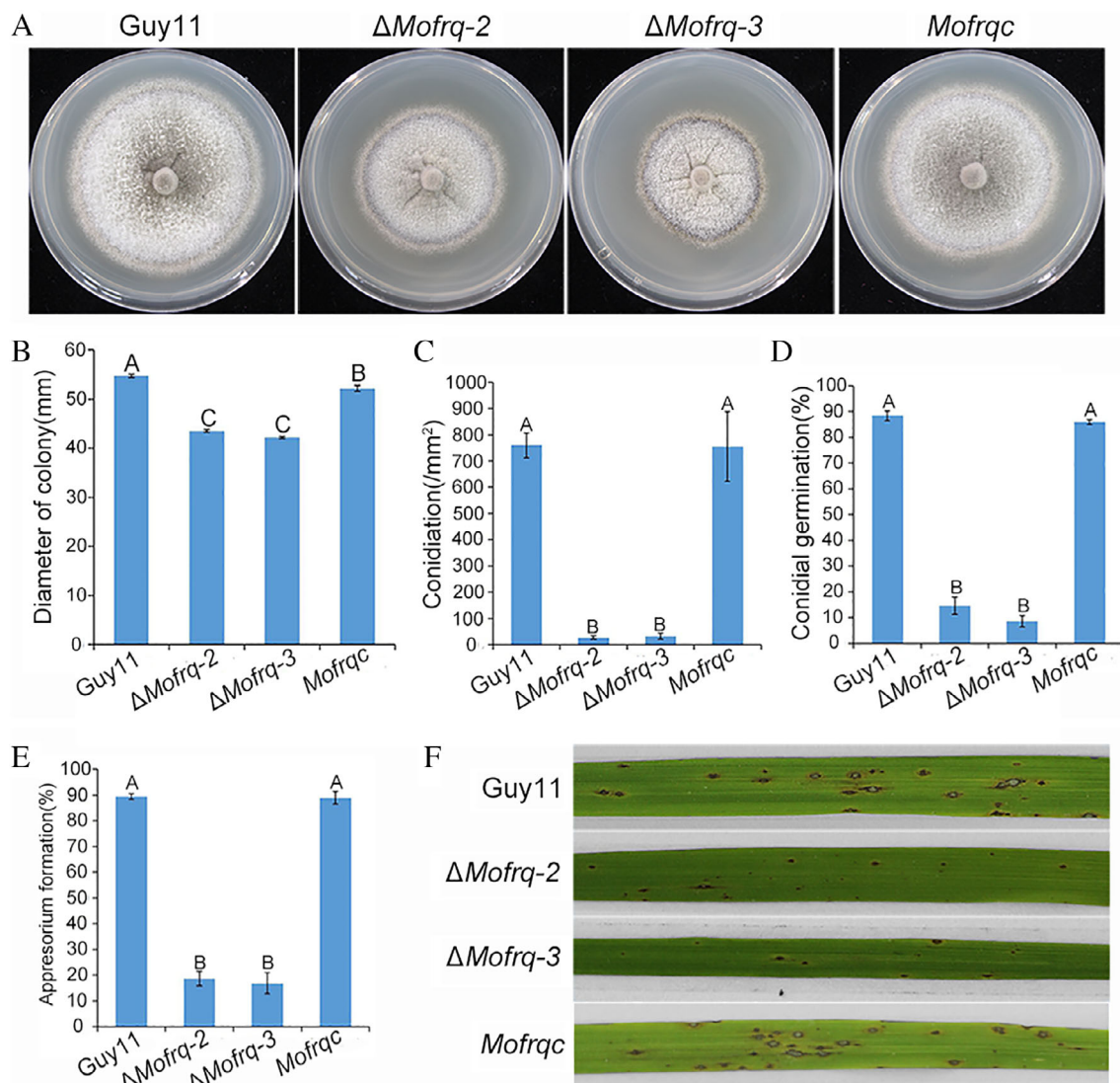

Fig. 7. Roles of *MoFRQ* in development and pathogenicity in *M. oryzae*. A. Growth of Guy11, two null mutants ΔMofrq-2, ΔMofrq-3 and complemented strain *Mofrqc* on a CM plate at 8 dpi. B. Diameters of the colonies were measured and presented. C. Conidiation of Guy11, two null mutants ΔMofrq-2, ΔMofrq-3 and complemented strain *Mofrqc*. D. Conidial germination of Guy11, two null mutants ΔMofrq-2, ΔMofrq-3 and complemented strain *Mofrqc* at 4 hpi. E. Appressorial formation of Guy11, two null mutants ΔMofrq-2, ΔMofrq-3 and the complemented strain *Mofrqc* at 24 hpi. Error bars represent standard deviation. Significant differences were displayed with different letters estimated by the Duncan' test ($P < 0.01$). F. Conidial suspensions (1×10^4) of Guy11, two null mutants ΔMofrq-2, ΔMofrq-3 and the complemented strain *Mofrqc* were sprayed on 2-week-old rice seedlings. Photographs were taken at 5 dpi. [Color figure can be viewed at wileyonlinelibrary.com]
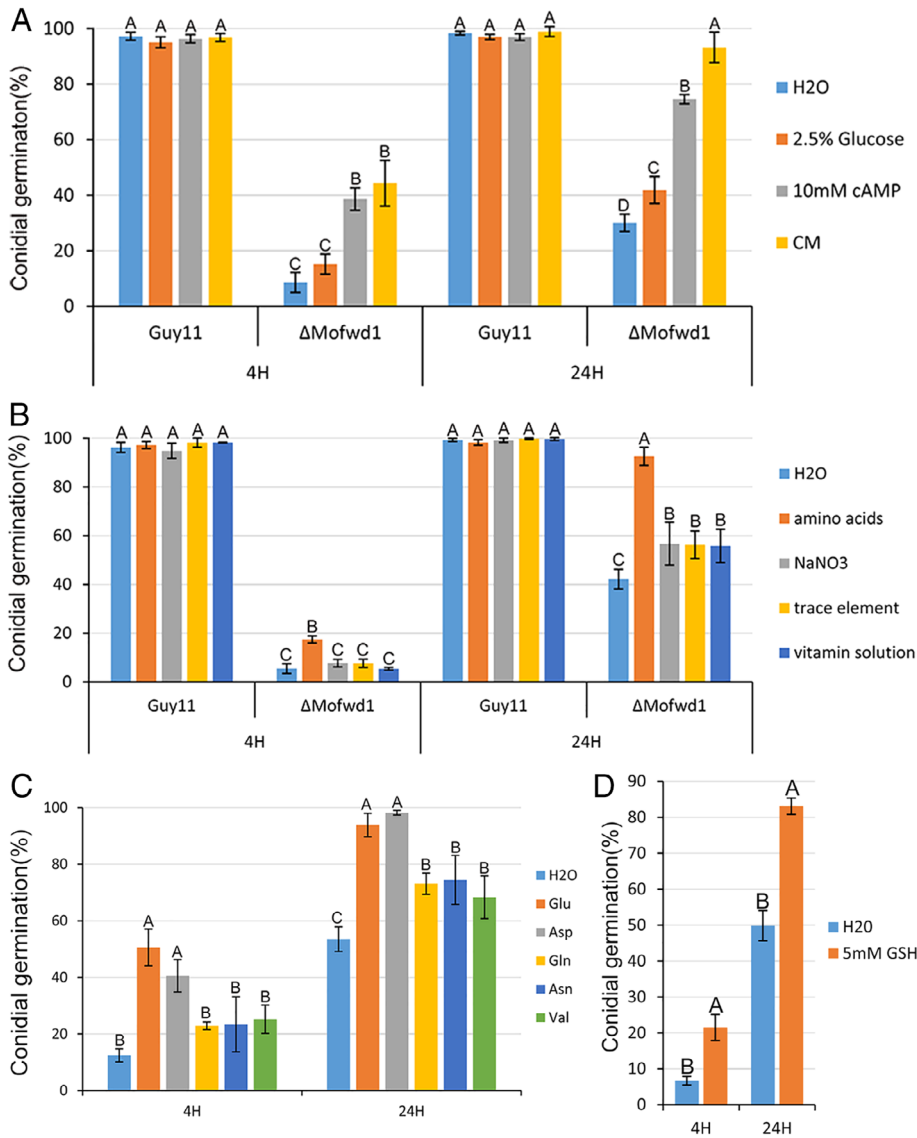
Fig. 8. Amino acids and reduced glutathione partially restored germination defects in ΔMofwd1. A. Effects of 2.5% glucose, 10 mM cAMP and complete medium on the conidial germination of Guy11 and Δ*Mofwd1* at 4 and 24 hpi. B. Effects on germination of the individual components of complete medium, including a mixture of 20 amino acids, sodium nitrate, trace elements, and vitamin solution at 4 and 24 hpi. C. Effects of glutamic acid, aspartic acid, glutamine, asparagine and valine on the germination of Δ*Mofwd1* at 4 and 24 hpi. D. Effect of glutathione on the spore germination of Δ*Mofwd1.* Sterile distilled water was used as the control. Error bars show standard deviation. No significant difference between ratios with the same letter estimated by Duncan's test ($P < 0.01$). [Color figure can be viewed at wileyonlinelibrary.com]

elements, vitamins, and distilled water alone, were used to suspend conidia from Guy11 and Δ*Mofwd1* respectively. As shown in Fig. 8B, only the amino acids solution significantly promoted the germination of Δ*Mofwd1* in contrast to the other four solutions at 4 hpi (17.5 ± 1.4%, 7.7 ± 1.6%, 7.6 ± 1.7%, 5.4 ± 0.5% and 5.5 ± 2.0% respectively). The germination percentage of Δ*Mofwd1* was restored to that of the wild type at 24 hpi (92.6 ± 3.7%). These data showed that amino acids played the largest role in stimulating Δ*Mofwd1* conidial germination among the components of the complete medium.

To further determine which amino acids could trigger germination of Δ*Mofwd1*, 20 common amino acids, each at a concentration of 0.05 g per litre, were used to test their respective roles in triggering Δ*Mofwd1* germination. Figure 8C shows that the germination ratios of Δ*Mofwd1* in

glutamic acid and aspartic acid were 50.6 ± 6.5% and 40.6 ± 5.7% at 4 hpi, higher than that in sterile distilled water (12.4 ± 2.3%). At 24 hpi, 5 amino acids of the 20 tested, including glutamic acid, aspartic acid, glutamine, asparagine and valine, increased the germination ratio of Δ*Mofwd1* (93.8 ± 4.1%, 98.2 ± 0.8%, 73.1 ± 3.8%, 74.4 ± 8.6% and 68.3 ± 7.5% respectively) in contrast to distilled water (53.5 ± 4.3) and the remaining 15 amino acids (Supporting Information Fig. S11). Glutamic acid and aspartic acid were the most effective of the amino acids tested. These data indicate that glutamic acid and aspartic acid are major triggers in restoring Δ*Mofwd1* germination.

The degradation of the glutamic acid pool in conidia plays a key role in producing reduced pyridine nucleotides in *N. crassa* (Foerster, 1972; Schmit and Brody, 1975). In *M. oryzae*, a highly reduced redox potential of glutathione

(GSH) is maintained during spore germination (Samalova *et al*., 2014). To determine whether the redox potential of GSH could rescue the germination defects in ∆*Mofwd1*, exogenous GSH was added into conidial drops of ∆*Mofwd1*. The germination ratios apparently increased from $6.7 \pm 1.2\%$ to $21.5 \pm 3.6\%$ at 4 hpi and from $49.8 \pm 4.2\%$ to $83.1 \pm 2.3\%$ at 24 hpi (Fig.8D), implicating a defect in the formation of reduced GSH in ∆*Mofwd1.*

Discussion

SCF complexes play important roles in controlling diverse biological and physiological processes in eukaryotic cells (Cardozo and Pagano, 2004; Liu and Xue, 2011). They modulate different regulatory and signalling pathways, especially in protein degradation dependent on different F-box proteins, which directly bind substrates and decide substrate specificity (Kipreos and Pagano, 2000). Here, we targeted 27 SCF complex-associated genes by a knockout strategy and successfully generated 21 F-box-containing gene disruptants. By systematically characterizing the 21 null mutants, we revealed that the F-box proteins MoFwd1, MoCdc4 and MoFbx15 play crucial roles in growth, development and virulence in the phytopathogenic fungus *M. oryzae.*

Recent studies highlighted the important roles of F-box proteins in fungal pathogenicity. Homologues of *S. cerevisiae* Grr1, extensively investigated in many fungi, have been found to be required for pathogenicity in *M. oryzae* (Sweigard *et al*., 1998; Guo *et al*., 2015), *F. graminearum* (Han *et al*., 2007), *F. oxysporum* (Miguel-Rojas and Hera, 2016), and *C. neoformans* (Liu *et al*., 2011). In our findings, pleiotropic functional defects in ∆*Mogrr1* were consistent with recent reports (Guo *et al*., 2015), while a reported role of Grr1 homologues in female fertility was further found to be conserved in *M. oryzae* (Han *et al*., 2007; Liu *et al*., 2011). Interestingly, another F-box protein, Frp1, showed a role in virulence in the plant-pathogenic fungi *F. oxysporum* (Duyvesteijn *et al*., 2005), *F. graminearum*, and *Botrytis cinerea* (Jonkers *et al*., 2011). In this study, among 21 F-box protein null mutants, ∆*Mofbx15*, ∆*Mocdc4* and ∆*Mofwd1* showed defects in full virulence, which could be explained by developmental defects in growth, asexual development, conidial germination, appressorial formation, appressorium-mediated or ALS-mediated penetration. Previous studies have shown that different regulation mechanisms are involved in controlling the formation of appressorium and appressorium-like structure in *M. oryzae* (Kong *et al*., 2013). Virulence differences of ∆*Mofbx15* due to hyphal or conidial-derived infection further suggest that MoFbx15 plays different roles in different infection mechanisms used by *M. oryzae*. Altogether, these data indicate that F-box proteins play multifunctional roles in the development of *M. oryzae* and can greatly influence the infection process.

Our data show that most of the cloned F-box proteins could participate in SCF complex formation in *M. oryzae*. Typical F-box proteins found in the SCF complex contain an N-terminal F-box domain and another substrate-binding domain in their C-terminal region (Jonkers and Rep, 2009). However, by SMART prediction, 15 of 24 F-box proteins did not contain other recognizable domains used for protein–protein interactions. In our study, 17 of 19 tested F-box proteins were found to interact with MoSkp1, except MoFbx15 and MGG_13660, further indicating that some F-box proteins may function in an SCF complex-independent manner or that interaction might be very transient and could not be proved by an Y2H assay. Similarly, in *S. cerevisiae*, Amn1, an F-box protein controlling the end of mitosis exit, does not bind Skp1 (Wang *et al*., 2003). Another F-box protein, Mfb1, regulates the dynamics of mitochondrial membrane fusion. Currently, there is no evidence demonstrating that it could bind Skp1 and no targets were identified (Durr *et al*., 2006). Therefore, MoFbx15 may function without forming an SCF complex. On the other hand, *A. fumigatus* Fbx15, a homologue of MoFbx15, was confirmed to interact with Skp1 using a bimolecular fluorescence complementation approach (Johnk *et al*., 2016). Thus, complementary approaches may be needed to determine the underlying molecular mechanisms.

The F-box domain is essential for F-box protein function because of its involvement in interaction with Skp1. In *S. cerevisiae*, F-box proteins have been well studied and most of them agree with the widely accepted model for F-box activity (Jonkers and Rep, 2009). In *N. crassa*, NcFwd1 lacking an F-box domain could not complement the defective growth and development of the disrupted mutant *fwd1*[RIP] (He *et al*., 2003). In *F. graminearum*, FgFbp1, an orthologue of ScGrr1, failed to interact with FgSkp1 when either the F-box domain or LRR domain was deleted. FgFbp1 lacking an F-box or LRR could not rescue defects in perithecia formation and virulence in ∆*Fgfbp1* (Liu *et al*., 2011). Our studies are also consistent with the current model because MoFwd1, MoCdc4 and MoGrr1 proteins lacking an F-box motif could not interact with MoSkp1. A pull-down assay between MoFwd1 and MoSkp1 further showed that the F-box domain participated directly in the interaction with MoSkp1. Additionally, MoFwd1, MoCdc4 and MoFbx15 lacking the F-box motif failed to restore growth, conidiation, conidial germination and full virulence. These data suggest that the F-box domain is necessary for functions of studied F-box proteins.

The exact transcriptional regulation and subcellular localization of F-box proteins are essential for their functions. In *A. fumigatus*, AfFbx15 with two putative NLS sites mainly accumulates in the nucleus in response to oxidative stress. In addition, AfFbx15 can regulate the transcriptional repressor Ssn6 in an SCF-independent

manner (Johnk *et al*., 2016). Comparably, MoFbx15 was also mobilized to the nucleus and highly expressed in invasive hyphae, suggesting a role in colonization and expansion in host cells. Microscopic observation of reduced ALS-mediated penetration and propagation in ∆*Mofbx15* was also consistent with this assumption. In *S. cerevisiae*, Cdc4 is located exclusively in the nucleus and required for G1/S and G2/M transitions in the cell cycle (Blondel *et al*., 2000). Our fluorescence microscopy observation displayed dotted nuclear localization of MoCdc4 in apical hyphae, where cell division is active, suggesting a possible role in the cell cycle. Involvement of MoCdc4 in conidial septation is also accordant with this postulation. In addition, deletion of the F-box domain did not disturb the localization of MoCdc4, further suggesting that the F-box domain was not involved in localization in some F-box proteins. In *N. crassa*, Frq is exported from the nucleus and degraded by Fwd1-mediated ubiquitination (Montenegro-Montero *et al*., 2015). The cytoplasmic localization of MoFwd1 supports this cellular process in *M. oryzae* as well.

The *M. oryzae* conidia germinate quickly into elaborate polarized germ tubes within 2 h after their attachment to hydrophobic surfaces (Wilson and Talbot, 2009). It is not easy to explore this biological process. Thus, the underlying mechanism by which the conidia switch from resting to activated state remains unclear. Recent evidence has shown that conidial germination is delayed by a proteasome inhibitor Bertomzib, indicating that the ubiquitin system plays a critical role in triggering germination (Oh *et al*., 2012). Our previous results identified an RING-type ubiquitin ligase MoUbr1 involved in activating conidial germination (Shi *et al*., 2016). In this study, we found that ∆*Mofbx15*, ∆*Mocdc4* and ∆*Mofwd1* also displayed obvious germination defects in different degrees, with ∆*Mofwd1* the most severe, suggesting that conidial germination is regulated by a complex network in which the ubiquitin system components take part.

Conidial germination is a fine-tuned process coordinated by environmental factors, signalling systems and metabolic processes (Osherov and May, 2001). The cAMP/PKA signalling pathway has been shown to play important roles in triggering germination. Deletion of *MAC1* adenylate cyclase caused delayed germination in *M. oryzae* (Choi and Dean, 1997). The exogenous addition of cAMP partially restored germination in ∆*Mofwd1*, implicating the participation of MoFwd1 in cAMP signalling. In *N. crassa*, amino acids, especially glutamic acid, were demonstrated to accumulate in conidia and decrease rapidly during the early stage of germination with production of NADH and NADPH, functioning in the reduction of oxidized glutathione during the initiation of germination (Schmit and Brody, 1975). Marketa *et al*. confirmed that *M. oryzae* conidia maintain a low level of

oxidation by the stable glutathione pools during early development (Samalova *et al*., 2014). In our study, exogenous amino acids, including glutamic acid, aspartic acid, glutamine, asparagine and valine, rescued delayed germination in ∆*Mofwd1*, implying that there are defects in amino acid pools in the ∆*Mofwd1* conidia. Furthermore, GSH restored the germination in ∆*Mofwd1.* These data indicated that a crosslink may exist between conidial amino acid metabolism and oxidative stress release. We hypothesize that MoFwd1 might be involved in the degradation of negative regulation factors required for amino acid synthesis. In *S. cerevisiae*, the F-box protein Cdc4 regulates the degradation of the transcriptional factor Gcn4, which activates the transcription of amino acid biosynthetic genes (Meimoun *et al*., 2000). Similar mechanisms may have also evolved for MoFwd1, although further experiments are needed to test this hypothesis.

The circadian clock is well studied in *N. crassa* and has been demonstrated to be controlled by negative feedback regulation. Rhythmic expression of *NcFRQ* was disrupted in ∆*Ncfwd1* (Montenegro-Montero *et al*., 2015). A recent report has confirmed that the transcription of *MoFRQ* displays a circadian rhythm in *M. oryzae* (Deng *et al*., 2015). Here, we found that the role of MoFwd1 was conserved in the regulation of circadian rhythm in *M. oryzae*. Although the rhythmic expression of *MoFRQ* is independent of MoFwd1, robust rhythmic expression of *MoFRQ* is necessary for the control of circadian rhythm in *M. oryzae.* MGWC1-1, a homologue of the *N. crassa* blue light receptor WC-1 (Froehlich *et al*., 2002), was confirmed to activate the expression of *MoFRQ* similarly to WC-1 (Kim *et al*., 2011). We thus hypothesized that the deletion of *MoFWD1* might cause accumulation of MoFrq, which resulted in inhibition on WC-1 and the further suppression of light-induced transcription of *MoFRQ*. The hypothesis was partially confirmed by the fact that the degradation of GFP-labelled MoFrq was impaired in ∆*Mofwd1. MoFRQ* was previously identified by a bidirectional genetic platform. An insertional mutant of *MoFRQ* displayed no apparent phenotypes except abnormal conidiophores (Park and Lee, 2013). In contrast, the deletion of *MoFRQ* caused slow growth, reduced conidiation, lower conidial germination and appressorial formation and reduced virulence in our work, indicating that *MoFRQ* is involved in development and differentiation in *M. oryzae.* We hypothesized that this discrepancy could be explained by several reasons. We deleted a genomic region, which was previously annotated as MGG_00903. Differently, the insertional mutant of *MoFRQ* had mutation in the C-terminal region only (Park and Lee, 2013).

In conclusion, our study provides insights into the important roles of F-box proteins MoFwd1, MoCdc4, MoFbx15 and MoGrr1 in growth, asexual and sexual development, conidial germination, appressorial formation and virulence

in *M. oryzae.* In detail, we highlights the regulatory roles of MoFwd1 in circadian response and conidial germination by its involvement in conidial amino acids accumulation, maintenance of a reduced state, cAMP signalling activation and the transcriptional and protein levels of *MoFRQ* (Fig. 9). Revealing the mechanisms underlying conidial germination in *M. oryzae* during plant infection will possibly identify fungal-specific targets to block the activation of germination. Insights into SCF-type ubiquitin ligase-mediated ubiquitination can contribute to developing new fungicides by focusing on the inhibition of germination and thus reducing crop production losses.

Materials and methods

Fungal strains and culture conditions

The strain Guy11 was used as the wild type in this study. The rice blast fungal strains were cultured on complete medium (CM) agar plates under 16 h of light and 8 h of dark at 25°C (Parker *et al.*, 2008). To observe the formation of asci and ascospores, the wild type (Mat1-2) and derivative mutant strains were crossed with the female strain 2539 (Mat1-1) on oatmeal medium at 25°C for 1 week and then transferred to constant fluorescent light for another 3 weeks of incubation at 22°C (Valent *et al.*, 1991).

Deletion and complementation of the SCF ubiquitin ligase-related genes

The knockout vectors were constructed as previously described (Lu *et al.*, 2014). Briefly, approximately 1.5 kb upstream and downstream flanking sequences of the target gene locus were cloned with specific primers (Supporting Information Table S1). The glufosinate resistance gene BAR (glufosinate acyltransferase) was amplified from pBARKS1 using the primers BAR-F/R. The resulting upstream and downstream DNA fragments and the BAR gene were fused together with XbaI/HindIII-linearized vector pKO1B catalysed with a one-step cloning kit (Vazyme Biotech Co. C113, China). After PCR verification, the correct knockout construct was transformed into Guy11 via *Agrobacterium tumefaciens*-mediated transformation (ATMT). Putative deletion transformants without green fluorescence were verified by PCR and Southern blotting. Southern blot analysis was performed with a digoxigenin (DIG) high prime DNA labelling and detection kit (Roche, Germany) following the manufacturer's instructions (Liu *et al.*, 2007). Genomic DNA was isolated from mycelia cultured in liquid CM for 2–3 days.

For complementation of the null mutant ΔMofwd1, the wild-type allele was amplified with the primers MoFwd1cF/MoFwd1cR (Supporting Information Table S1) and ligated to EcoRI/BamHI-digested vector pKD5 (Chen *et al.*, 2013), which carries the sulfonylurea resistance gene. The resulting vector was verified by PCR and reintroduced into null mutant ΔMofwd1 by ATMT. The transformants were screened on DCM media (10 g/l glucose, 2 g/l asparagine, 1.7 g/l yeast nitrogen base without amino acid, 1 g/l NH$_4$NO$_3$, and 15 g/l agar, pH 6.0 adjusted with NaH$_2$PO$_4$) with 100 μg ml^{-1} sulfonylurea. Similar strategies were adopted to complement ΔMocdc4 and ΔMofbx15.

To perform the domain complementation analysis of the F-box proteins MoFwd1, MoFbx15 and MoCdc4, mutants lacking the F-box domain were constructed. To construct MoFwd1ΔF, two fragments flanking the F-box domain were amplified from the coding sequence of MoFwd1 with the primers MoFwd1F/Fwd1ΔF-1R and Fwd1ΔF-2F/Fwd1R. The resulting two DNA fragments and the 2-kb native promoter amplified with Fwd1proF/Fwd1proR were then fused with EcoRI/BamHI-digested plasmid pKD5. After sequencing, the construct was transformed into ΔMofwd1. The
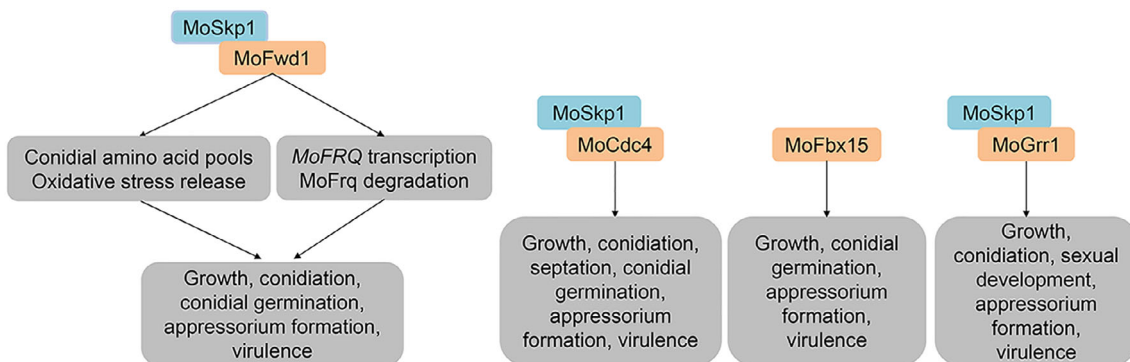

Fig. 9. Proposed model of virulence-related roles for F-box proteins in *M. oryzae*. MoFwd1 regulates growth, conidiation, conidial germination, appressorium formation, virulence by affecting the accumulation of conidial amino acid pools, oxidative stress release, *MoFRQ* transcription and MoFrq degradation; MoCdc4 regulates growth, conidiation, septation, conidial germination, appressorium formation, and virulence; MoFbx15 regulates conidial germination, appressorium formation, and virulence; MoGrr1 regulates growth, conidiation, sexual development, appressorium formation and virulence. [Color figure can be viewed at wileyonlinelibrary.com]

same strategy was adopted to delete the F-box domain of MoFbx15 and MoCdc4. The primers used in this part are listed in the Supporting Information Table S1.

Growth, conidiation, conidial germination and appressorial formation assays

For growth and asexual conidiation evaluation, Guy11 and derivative strains were cultured on CM plates under 16 h of light and 8 h of dark at 25°C and measured at 7 days post inoculation (dpi). The conidial length and width of different strains were surveyed on more than 200 conidia. The differentiation of conidiophores and conidia were observed as described previously in a culture chamber with constant light (Lau and Hamer, 1998). To compare the differences in spore germination and appressorium formation, 40 μl of conidial suspension (1×10^5 conidia/ml) were inoculated onto a hydrophobic plastic surface and over 100 conidia were investigated at 4 and 24 hpi. To examine the effects of amino acids and glutathione on the conidial germination of ΔMofwd1, 20 amino acids were added into conidial drops of ΔMofwd1 together or individually at a concentration of 0.05 g per litre and reduced glutathione was used at 5 mM. The assays were repeated independently three times, each time with three replicates.

Plant infection assays

Appressorium-mediated or appressorium-like structure-mediated penetration and invasive growth were monitored as previously described (Kong *et al*., 2013). Twenty microliters of conidial suspension (5×10^4 conidia/ml) were inoculated onto barley leaf surfaces (Golden Promise), which were then decoloured and observed at 48 hpi (Cao *et al*., 2018). All experiments that were analysed statistically were repeated independently three times, each time with three replicates.

For the plant infection assays, 5 mm diameter mycelial agar plugs were laid on the barley leaves at 25°C under moist conditions, and the results were photographed at 4–5 dpi. Two millilitres of conidial solution, diluted to 1×10^5 conidia/ml with 0.2% gelatin, were sprayed on three to four leaf stage rice seedlings prior to screening for the virulence phenotype. Rice leaves were photographed 5 days after spray inoculation (Lu *et al*., 2014).

Quantitative RT-PCR assay

Total RNA was extracted using an RNAiso kit (TaKaRa, Japan) according to the manufacturer's instructions. To explore the gene profiles of *MoCDC4*, *MoFWD1* and *MoFBX15*, five developmental stages of the wild-type strain were sampled including mycelia cultured in CM, conidia, appressoria at 18 hpi, infected rice leaves at 4 dpi, and nitrogen-starved mycelia (Liu *et al*., 2016). To

determine the gene expression of the circadian clock-related gene *MoFRQ*, the wild-type strain and ΔMofwd1 were cultured in liquid CM for 3 days in the dark, induced by light for 30 min, and then cultured for another 48 h under a cycle of 12 h dark and 12 h light or cultured in constant darkness. Samples were collected every 4 h. Single-strand cDNA was synthesized with a reverse transcription kit (TaKaRa, Japan). Quantitative RT-PCR assays were performed with SYBR Premix Ex Taq (TaKaRa, Japan) on a Mastercycler ep Realplex thermal cycler (Eppendorf). Relative transcript abundance was calculated by the $2^{-\Delta\Delta Ct}$ method and normalized with β-tubulin (Livak and Schmittgen, 2001). The qPCR experiment was repeated at least twice independently, with each sample run in triplicate, and a representative data set was shown. Primers used for probing each gene are listed in the Supporting Information Table S1.

Yeast two-hybrid assay

The yeast two-hybrid assay was performed as stated in the manual for the BD Matchmaker Library Construction & Screening Kit (Clontech, USA). The coding sequences of the F-box genes were cloned with primers listed in Table S1 from mycelial or appressorial cDNA libraries of Guy11 and then ligated into prey vector pGADT7 digested by EcoRI/BamHI. MoSkp1 was cloned into bait vector pGBKT7 digested by EcoRI/BamHI or into prey vector pGADT7. To construct MoCdc4 lacking an F-box domain, flanking fragments of the F-box were cloned from the MoCdc4 coding sequence with primers MoCdc4BD-F/MoCdc4ΔFBD-1R and MoCdc4ΔFBD-2F/ MoCdc4BD-R, and then ligated into EcoRI/BamHI-digested pGADT7 with a one-step cloning kit (Vazyme Biotech Co. C113, China). Similar strategies were chosen to generate other bait constructs, including MoCdc4 and MoFwd1 and MoGrr1 lacking either the F-box, WD40 or LRR domains. Pairwise combinations of prey and bait constructs were cotransformed into the yeast strain AH109 following verification by sequencing. The resulting yeast cells grown on the auxotrophic medium SD-Leu-Trp were diluted to 1×10^6 ml^{-1} and dropped on SD-Leu-Trp-Ade-His medium for growth before photographs were taken. Positive and negative controls were from the kit. Yeast total proteins were extracted with a yeast total protein extraction kit (Sangon, C500013). Expression of the fusion proteins was detected by a western blotting using anti-HA antibody (Abbkine) or anti-cMyc antibody (Clontech).

Fluorescent-microscopy observation

To validate the subcellular localization of MoFwd1, the ORF of MoFwd1 was cloned from plasmid pGADT7-MoFwd1 with primers listed in the Supporting Informtion Table S1 and ligated into pKD5-GFP (Chen *et al*., 2013) digested by

XbaI/SalI to generate pKD5GFP-MoFwd1. After the GFP-MoFwd1 fusion construct was sequenced to confirm the correct coding framework, the vector was transformed into Δ*Mofwd1.* To observe the localization of MoFbx15 and MoCdc4, the coding sequences of *MoFBX15* and *MoCDC4* were inserted into plasmid pKD5GFP digested with BamHI/SmaI to form pKD5MoFbx15GFP and pKD5MoCdc4GFP, which were then transformed into the null mutants Δ*Mofbx15* and Δ*Mocdc4* respectively. Rescued transformants with GFP signals were observed and documented by confocal laser scanning microscopy using a Zeiss LSM780. Mycelial samples and appressoria were prepared as previously described by incubating conidia in liquid CM for 24 h to form hyphae or by incubating conidia on hydrophobic films to induce appressorial formation at 25°C. Samples were stained with 100 μg ml^{-1} Hoechst 33342 (Sigma, USA) for 30 min to label nuclei for micrographs. To observe the localization of MoFwd1 in planta during infection, conidia drops were inoculated into 4-week-old rice sheath and monitored at 48 hpi.

To detect MoFrq degradation, the coding sequence of *MoFRQ* was cloned with primers GFPMoFRQF/GFPMoFRQR and ligated into XbaI/SalI-digested pKD5-GFP. The resultant construct was transformed into Guy11 and Δ*Mofwd1.* The expression of MoFrq was monitored by qPCR. Protein extraction and western blotting were performed as previously described (Shi *et al.*, 2016).

Coimmunoprecipitation assay

To detect the interaction between MoSkp1 and MoFwd1, MoSkp1 was cloned with primers Skp1FlagF/Skp1FlagR (Supporting Information Table S1) and inserted into pKD7-3 × Flag carrying a histone 3 promoter. Subsequently, the MoSkp1-3Flag construct was introduced into transformant expressing GFP-MoFwd1, which was previously used for observing localization of MoFwd1. Total protein was extracted with protein extraction buffer (10 mM Tris–HCl, pH 7.5, 150 mM NaCl, 0.5 mM EDTA, 1% TritonX-100) supplemented with 1 mM PMSF and protease inhibitor cocktail (ThermoFisher, USA). A piece of GFP-Trap beads (chromotek, Germany) was incubated with the total protein supernatant at 4°C for 4 h and then washed with wash buffer (10 mM Tris/HCl pH 7.5, 150 mM NaCl, 0.5 mM EDTA) three times, finally eluted with elution buffer (0.2 mM Glycine pH 2.5). The eluted protein solution was subjected to SDS-PAGE and transferred to a PVDF membrane. Primary antibodies including anti-Flag antibody (Sigma) and anti-GFP antibody (Sigma), with a peroxidase (HRP)-conjugated secondary antibody (HUABIO, China) were used as previously reported. An ECL chemiluminescent kit (BioRad, USA) was used for western blot detection.

GST pull-down assay

The cDNA fragments encoding MoSkp1, MoFwd1ΔF-box and MoFwd1ΔWD40 were amplified and inserted into pGEX4T-1 or pET21a, respectively, to generate GST-MoSkp1, His-MoFwd1ΔF-box and His-MoFwd1ΔWD40 fusion constructs. The resultant constructs were transformed into *E. coli* BL21 (DE3) cells, which were then cultured at 37°C and induced at 18°C overnight with 0.1 mM IPTG (isopropyl β-D-thiogalactopyranoside). Five millilitres of bacterial cultures were collected and suspended in lysis buffer (50 mM Tris, 0.2 M NaCl, 3% glycerol, and 1 mM PMSF, pH 7.5). After ultrasonic fragmentation, bacteria lysates expressing GST and GST-MoSkp1 were incubated with 50 μl glutathione beads according to GST Sefinose resin kit (Sangon, China). The beads were washed five times with lysis buffer before they were incubated with lysates expressing His-MoFwd1ΔF-box and His-MoFwd1ΔWD40. After incubation of another 2 h at 25°C, the beads were washed again five times with wash buffer (50 mM Tris/HCl pH 8.0, 0.5 mM NaCl, 5 mM EDTA, 1% Triton X-100) and eluted with elution buffer (10 mM GSH, 50 mM Tris/HCl pH 8.0). The recombinant proteins were detected with anti-GST antibody and anti-His antibody (HUABIO, China) by western blotting.

References

Ardley, H.C., and Robinson, P.A. (2005) E3 ubiquitin ligases. *Essays Biochem* **41**: 15–30.

Atir-Lande, A., Gildor, T., and Kornitzer, D. (2005) Role for the SCFCDC4 ubiquitin ligase in *Candida albicans* morphogenesis. *Mol Biol Cell* **16**: 2772–2785.

Blondel, M., Galan, J.M., Chi, Y., Lafourcade, C., Longaretti, C., Deshaies, R.J., and Peter, M. (2000) Nuclear-specific degradation of Far1 is controlled by the localization of the F-box protein Cdc4. *EMBO J* **19**: 6085–6097.

Bourett, T.M., and Howard, R.J. (1990) *In vitro* development of penetration structures in the rice blast fungus *Magnaporthe grisea. Can J Bot* **68**: 329–342.

Callis, J. (2014) The ubiquitination machinery of the ubiquitin system. *Arabidopsis Book* **12**: e0174.

Cao, H., Huang, P., Yan, Y., Shi, Y., Dong, B., Liu, X., *et al*. (2018) The basic helix-loop-helix transcription factor Crf1 is required for development and pathogenicity of the rice blast fungus by regulating carbohydrate and lipid metabolism. *Environ Microbiol* **20**: 3427–3441.

Cardozo, T., and Pagano, M. (2004) The SCF ubiquitin ligase: insights into a molecular machine. *Nat Rev Mol Cell Biol* **5**: 739–751.

Chen, G., Liu, X., Zhang, L., Cao, H., Lu, J., and Lin, F. (2013) Involvement of *MoVMA11*, a putative vacuolar ATPase c' subunit, in vacuolar acidification and infection-related morphogenesis of *Magnaporthe oryzae*. *PLoS One* **8**: e67804.

Choi, W., and Dean, R.A. (1997) The adenylate cyclase gene *MAC1* of *Magnaporthe grisea* controls appressorium formation and other aspects of growth and development. *Plant Cell* **9**: 1973–1983.

Colabardini, A.C., Humanes, A.C., Gouvea, P.F., Savoldi, M., Goldman, M.H.S., Kress, M.R.v.Z., *et al*. (2012) Molecular characterization of the *Aspergillus nidulans fbxA* encoding an F-box protein involved in xylanase induction. *Fungal Genet Biol* **49**: 130–140.

Deng, Y.Z., Qu, Z., and Naqvi, N.I. (2015) Twilight, a novel circadian-regulated gene, integrates phototropism with nutrient and redox homeostasis during fungal development. *PLoS Pathog* **11**: e1004972.

Durr, M., Escobar-Henriques, M., Merz, S., Geimer, S., Langer, T., and Westermann, B. (2006) Nonredundant roles of mitochondria-associated F-box proteins Mfb1 and Mdm30 in maintenance of mitochondrial morphology in yeast. *Mol Biol Cell* **17**: 3745–3755.

Duyvesteijn, R.G.E., van Wijk, R., Boer, Y., Rep, M., Cornelissen, B.J.C., and Haring, M.A. (2005) Frp1 is a *Fusarium oxysporum* F-box protein required for pathogenicity on tomato. *Mol Microbiol* **57**: 1051–1063.

Ebbole, D.J. (2007) *Magnaporthe* as a model for understanding host-pathogen interactions. *Annu Rev Phytopathol* **45**: 437–456.

Elert, E. (2014) Rice by the numbers: a good grain. *Nature* **514**: S50–S51.

Foerster, H.F. (1972) Spore pool glutamic acid as a metabolite in germination. *J Bacteriol* **111**: 437–442.

Froehlich, A.C., Liu, Y., Loros, J.J., and Dunlap, J.C. (2002) White Collar-1, a circadian blue light photoreceptor, binding to the frequency promoter. *Science* **297**: 815–819.

Glickman, M.H., and Ciechanover, A. (2002) The ubiquitin-proteasome proteolytic pathway: destruction for the sake of construction. *Physiol Rev* **82**: 373–428.

Goh, P.Y., and Surana, U. (1999) Cdc4, a protein required for the onset of S phase, serves an essential function during G(2)/M transition in *Saccharomyces cerevisiae*. *Mol Cell Biol* **19**: 5512–5522.

Guo, M., Gao, F., Zhu, X., Nie, X., Pan, Y., and Gao, Z. (2015) MoGrr1, a novel F-box protein, is involved in conidiogenesis and cell wall integrity and is critical for the full virulence of *Magnaporthe oryzae*. *Appl Microbiol Biotechnol* **99**: 8075–8088.

Han, Y.-K., Kim, M.-D., Lee, S.-H., Yun, S.-H., and Lee, Y.-W. (2007) A novel F-box protein involved in sexual development and pathogenesis in *Gibberella zeae*. *Mol Microbiol* **63**: 768–779.

He, Q., Cheng, P., Yang, Y., He, Q., Yu, H., and Liu, Y. (2003) FWD1-mediated degradation of FREQUENCY in *Neurospora* establishes a conserved mechanism for circadian clock regulation. *EMBO J* **22**: 4421–4430.

Howard, R.J., Ferrari, M.A., Roach, D.H., and Money, N.P. (1991) Penetration of hard substrates by a fungus employing enormous turgor pressures. *Proc Natl Acad Sci U S A* **88**: 11281–11284.

Johnk, B., Bayram, O., Abelmann, A., Heinekamp, T., Mattern, D.J., Brakhage, A.A., *et al*. (2016) SCF ubiquitin ligase F-box protein Fbx15 controls nuclear co-repressor localization, stress response and virulence of the human pathogen *Aspergillus fumigatus*. *PLoS Pathog* **12**: e1005899.

Jonkers, W., and Rep, M. (2009) Lessons from fungal F-box proteins. *Eukaryot Cell* **8**: 677–695.

Jonkers, W., Van Kan, J.A.L., Tijm, P., Lee, Y.-W., Tudzynski, P., Rep, M., and Michielse, C.B. (2011) The FRP1 F-box gene has different functions in sexuality, pathogenicity and metabolism in three fungal pathogens. *Mol Plant Pathol* **12**: 548–563.

Kim, S., Singh, P., Park, J., Park, S., Friedman, A., Zheng, T., *et al*. (2011) Genetic and molecular characterization of a blue light photoreceptor MGWC-1 in *Magnaporth oryzae*. *Fungal Genet Biol* **48**: 400–407.

Kipreos, E.T., and Pagano, M. (2000) The F-box protein family. *Genome Biol* **1**: REVIEWS3002.

Kong, L.-A., Li, G.-T., Liu, Y., Liu, M.-G., Zhang, S.-J., Yang, J., *et al*. (2013) Differences between appressoria formed by germ tubes and appressorium-like structures developed by hyphal tips in *Magnaporthe oryzae*. *Fungal Genet Biol* **56**: 33–41.

Krappmann, S., Jung, N., Medic, B., Busch, S., Prade, R.A., and Braus, G.H. (2006) The *Aspergillus nidulans* F-box protein GrrA links SCF activity to meiosis. *Mol Microbiol* **61**: 76–88.

Lau, G.W., and Hamer, J.E. (1998) Acropetal: a genetic locus required for conidiophore architecture and pathogenicity in the rice blast fungus. *Fungal Genet Biol* **24**: 228–239.

Li, W., Bengtson, M.H., Ulbrich, A., Matsuda, A., Reddy, V. A., Orth, A., *et al*. (2008) Genome-wide and functional annotation of human E3 ubiquitin ligases identifies MULAN, a mitochondrial E3 that regulates the organelle's dynamics and signaling. *PLoS One* **3**: e1487.

Liu, T.-B., and Xue, C. (2011) The ubiquitin-proteasome system and F-box proteins in pathogenic fungi. *Mycobiology* **39**: 243–248.

Liu, T.-B., and Xue, C. (2014) Fbp1-mediated ubiquitin-proteasome pathway controls *Cryptococcus neoformans* virulence by regulating fungal intracellular growth in macrophages. *Infect Immun* **82**: 557–568.

Liu, T.-B., Wang, Y., Stukes, S., Chen, Q., Casadevall, A., and Xue, C. (2011) The F-Box protein Fbp1 regulates sexual reproduction and virulence in *Cryptococcus neoformans*. *Eukaryot Cell* **10**: 791–802.

Liu, X.-H., Ning, G.-A., Huang, L.-Y., Zhao, Y.-H., Dong, B., Lu, J.-P., and Lin, F.-C. (2016) Calpains are involved in asexual and sexual development, cell wall integrity and pathogenicity of the rice blast fungus. *Sci Rep* **6**: 31204.

Liu, X.H., Lu, J.P., Zhang, L., Dong, B., Min, H., and Lin, F. C. (2007) Involvement of a *Magnaporthe grisea* serine/-threonine kinase gene, *MgATG1*, in appressorium turgor and pathogenesis. *Eukaryot Cell* **6**: 997–1005.

Livak, K.J., and Schmittgen, T.D. (2001) Analysis of relative gene expression data using real-time quantitative PCR and the 2(−Delta Delta C(T)) method. *Methods* **25**: 402–408.

Lu, J., Cao, H., Zhang, L., Huang, P., and Lin, F. (2014) Systematic analysis of Zn2Cys6 transcription factors required for development and pathogenicity by high-throughput

gene knockout in the rice blast fungus. *PLoS Pathog* **10**: e1004432.

Meimoun, A., Holtzman, T., Weissman, Z., McBride, H.J., Stillman, D.J., Fink, G.R., and Kornitzer, D. (2000) Degradation of the transcription factor Gcn4 requires the kinase Pho85 and the SCF(CDC4) ubiquitin-ligase complex. *Mol Biol Cell* **11**: 915–927.

Miguel-Rojas, C., and Hera, C. (2016) The F-box protein Fbp1 functions in the invasive growth and cell wall integrity mitogen-activated protein kinase (MAPK) pathways in *Fusarium oxysporum*. *Mol Plant Pathol* **17**: 55–64.

Montenegro-Montero, A., Canessa, P., and Larrondo, L.F. (2015) Around the fungal clock: recent advances in the molecular study of circadian clocks in *Neurospora* and other fungi. *Adv Genet* **92**: 107–184.

Oh, Y., Franck, W.L., Han, S.-O., Shows, A., Gokce, E., Muddiman, D.C., and Dean, R.A. (2012) Polyubiquitin is required for growth, development and pathogenicity in the rice blast fungus *Magnaporthe oryzae*. *PLoS One* **7**: e42868.

Oh, Y., Donofrio, N., Pan, H., Coughlan, S., Brown, D.E., Meng, S., *et al*. (2008) Transcriptome analysis reveals new insight into appressorium formation and function in the rice blast fungus *Magnaporthe oryzae*. *Genome Biol* **9**: R85.

Osherov, N., and May, G.S. (2001) The molecular mechanisms of conidial germination. *FEMS Microbiol Lett* **199**: 153–160.

Park, J., and Lee, Y.-H. (2013) Bidirectional-genetics platform, a dual-purpose mutagenesis strategy for filamentous fungi. *Eukaryot Cell* **12**: 1547–1553.

Parker, D., Beckmann, M., Enot, D.P., Overy, D.P., Rios, Z.C., Gilbert, M., *et al*. (2008) Rice blast infection of *Brachypodium distachyon* as a model system to study dynamic host/pathogen interactions. *Nat Protoc* **3**: 435–445.

Prakash, C., Manjrekar, J., and Chattoo, B.B. (2016) Skp1, a component of E3 ubiquitin ligase, is necessary for growth, sporulation, development and pathogenicity in rice blast fungus (*Magnaporthe oryzae*). *Mol Plant Pathol* **17**: 903–919.

Samalova, M., Meyer, A.J., Gurr, S.J., and Fricker, M.D. (2014) Robust anti-oxidant defences in the rice blast fungus *Magnaporthe oryzae* confer tolerance to the host oxidative burst. *New Phytol* **201**: 556–573.

Schmit, J.C., and Brody, S. (1975) *Neurospora crassa* conidial germination: role of endogenous amino acid pools. *J Bacteriol* **124**: 232–242.

Shi, H.-B., Chen, G.-Q., Chen, Y.-P., Dong, B., Lu, J.-P., Liu, X.-H., and Lin, F.-C. (2016) MoRad6-mediated ubiquitination pathways are essential for development and pathogenicity in *Magnaporthe oryzae*. *Environ Microbiol* **18**: 4170–4187.

Skamnioti, P., and Gurr, S.J. (2009) Against the grain: safeguarding rice from rice blast disease. *Trends Biotechnol* **27**: 141–150.

Su, N.Y., Flick, K., and Kaiser, P. (2005) The F-box protein Met30 is required for multiple steps in the budding yeast cell cycle. *Mol Cell Biol* **25**: 3875–3885.

Sweigard, J.A., Carroll, A.M., Farrall, L., Chumley, F.G., and Valent, B. (1998) *Magnaporthe grisea* pathogenicity genes obtained through insertional mutagenesis. *MPMI* **11**: 404–412.

Takano, Y., Choi, W., Mitchell, T.K., Okuno, T., and Dean, R.A. (2003) Large scale parallel analysis of gene expression during infection-related morphogenesis of *Magnaporthe grisea*. *Mol Plant Pathol* **4**: 337–346.

Talbot, N.J. (1995) Having a blast: exploring the pathogenicity of *Magnaporthe grisea*. *Trends Microbiol* **3**: 9–16.

Talbot, N.J. (2003) On the trail of a cereal killer: exploring the biology of *Magnaporthe grisea*. *Annu Rev Microbiol* **57**: 177–202.

Tucker, S.L., and Talbot, N.J. (2001) Surface attachment and pre-penetration stage development by plant pathogenic fungi. *Annu Rev Phytopathol* **39**: 385–417.

Valent, B., Farrall, L., and Chumley, F.G. (1991) *Magnaporthe grisea* genes for pathogenicity and virulence identified through a series of backcrosses. *Genetics* **127**: 87–101.

Wang, Y., Shirogane, T., Liu, D., Harper, J.W., and Elledge, S.J. (2003) Exit from exit: resetting the cell cycle through Amn1 inhibition of G protein signaling. *Cell* **112**: 697–709.

Wilson, R.A., and Talbot, N.J. (2009) Under pressure: investigating the biology of plant infection by *Magnaporthe oryzae*. *Nat Rev Microbiol* **7**: 185–195.

Supporting Information

Additional Supporting Information may be found in the online version of this article at the publisher's web-site:

Fig. S1. Detection of fusion proteins in yeast transformants. Partial fusion proteins were detected for expression in yeast.

Fig. S2. Verification of deletion mutants by PCR and Southern blotting. (A) Double PCR test of the null mutants including amplification of a gene inner fragment and the fragment after genomic recombination. (B) and (C) Southern blotting of 14 F-box-related gene mutants. Knockout strategies were shown with probes and restriction enzymes used in Southern blotting. Different lengths of the bands were displayed in Guy11 and null mutants.

Fig. S3. Pathogenicity of strains on barley leaves. Mycelial plugs of various strains including Guy11 and the 21 F-box protein deleted mutants were inoculated on barley leaves. The results were photographed at 5 dpi.

Fig. S4. Proportion of the lesion area on rice leaves. Error bars indicate standard deviation. The data were analysed by Duncan's test ($P < 0.01$); columns labelled with same letter do not differ significantly.

Fig. S5. Conidial septation in Guy11, Δ*Mocdc4* and the complemented strain. Numbers of septa per conidium were counted in more than 100 conidia stained with CFW.

Fig. S6. F-box protein MoGrr1 was important for female fertility. Various couples of opposite mating-type strains were crossing cultured on OMA medium under light. Asci and ascospores were observed at four weeks post inoculation. Bar = 50 μm.

Fig. S7. Expression of F-box genes in Guy11, domain deletion-complemented mutants, and complemented strains. The data were analysed by Duncan's test ($P < 0.01$), columns labelled with the same letter have no significant difference.

Fig. S8. MoFbx15 was located in the nucleus during development of the appressorium. Bar = 10 μm. The fluorescence was observed at conidial, germinated, appressorial stages.

Fig. S9. Fluorescent localization of MoFwd1 during invasive stage in rice sheath. The pictures were taken 48 hpi. Bar = 10 μm.

Fig. S10. Phenotypic changes of strain Δ*Mofwd1* constitutively expressing GFP-MoFrq. Basic phenotypic were evaluated by measuring colony diameter at 8 dpi,

conidiation at 8 dpi, conidial germination at 4 hpi, appressorium formation at 24 hpi and virulence on barley leaves at 4 dpi.

Fig. S11. Germination rates of Δ*Mofwd1* conidia incubated with other amino acids. No significant difference was observed at 4 hpi and 24 hpi for these 15 kinds of amino acids.

Table S1. Primers used in this study.

Table S2. Summary of SCF-associated gene deletions.

Table S3. Phenotypic data of F-box domain deletion mutants.